Coordination Chemistry Reviews 255 (2011) 1603–1622

Contents lists available at ScienceDirect

Coordination Chemistry Reviews

journal homepage: www.elsevier.com/locate/ccr

Review

Hexamethylenetetramine: An old new building block for design of coordination polymers

Alexander M. Kirillov*

Centro de Química Estrutural, Complexo I, Instituto Superior Técnico, TU Lisbon, Av. Rovisco Pais, 1049-001 Lisbon, Portugal

Contents

ARTICLE INFO

Article history:
Received 6 October 2010
Accepted 7 January 2011
Available online 15 January 2011

Keywords:
Hexamethylenetetramine (hmt)
Crystal engineering
Metal-organic frameworks (MOFs)
Self-assembly
Coordination chemistry
Supramolecular structures
Water clusters
Magnetic properties
Photoluminescence

ABSTRACT

The design of new coordination polymers is nowadays a challenging research topic that attracts increasing interest due to the unique structural and functional properties of such metal-organic materials. In contrast to the recognized use of some N-donor ligands for the construction of coordination polymers, the application of hexamethylenetetramine (hmt) as a simple, commercially available, water-soluble and highly versatile cagelike building block has so far been explored to a lesser extent, although a considerable number of hmt-driven metal-organic networks have been reported in the last few years. Given the high potential of hmt for future developments of this research field, the present review summarizes the main structural and topological types of coordination polymers bearing hmt. These compounds feature a high diversity of topologies that include linear, zigzag, double, triple and quadruple 1D chains, rectangular grids, flat and undulating 2D layers, as well as layer-pillared, octahedral, zeolite-like, honeycomb-like and other complex 3D nets, in which hmt acts as a linker or spacer, pillar or connector, stabilizer and/or supporting ligand. The most common synthetic strategies are reviewed, showing that a diversity of metal-organic networks can be generated by facile self-assembly routes in aqueous medium and using rather simple chemicals. The main types of auxiliary ligands necessary for the construction of hmt-driven coordination networks are also identified. The additional structural features such as the formation

Abbreviations: 1D, one-dimensional; 2D, two-dimensional; 3D, three-dimensional; ac, acetate; adca, adamantane-1-carboxylate; alhmt, N-allyl-hexamethylenetetramine(1+); bpbpd, 1,1′-biphenyl-4,4′-diylbis(4,4-dimethylpentane-1,3-dione); ctc, *cis,cis*-1,3,5-cyclohexanetricarboxylate; dabco, 1,4-diazabicyclo[2.2.2]octane (triethylenediamine); dca, dicyanamide; DMA, dimethylacetamide; DMF, dimethylformamide; dpa, 2,2′-biphenyldicarboxylate; dtb, 2,2′-dithiodibenzoate; fba, 4-formylbenzoate; HE, high energy; hmt, hexamethylenetetramine; hmtH, monoprotonated hmt; ibut, isobutyrate; LE, low energy; LMCT, ligand-to-metal charge transfer; M:hmt, metal-to-hmt molar ratio; mal, malonate; male, maleate; MTN, zeolite socony mobil–thirty-nine; nita, 7-nitro-1,3,5-triaza-adamantane; nta, nitrilotriacetate; opbh, 2-oxopropionate(benzoyl)hydrazone; pbhd, 1,1′-(1,4-phenylene)-bis(hexane-1,3-dione); pbpd, 1,1′-(1,3-phenylene)-bis(4,4-dimethylpentane-1,3-dione); pdc, 3,4-pyridinedicarboxylate; phac, phenylacetate; phca, phenanthrene-9-carboxylate; pma, pyromellitate (1,2,4,5-benzenetetracarboxylate); prop, propionate; pta, 1,3,5-triaza-7-phosphaadamantane; ptao, 1,3,5-triaza-7-phospha-adamantane-7-oxide; ptas, 1,3,5-triaza-7-phospha-adamantane-7-sulfide; r.t., room temperature; sh., shoulder; tar, L-tartrate; tcm, tricyanomethanide; THF, tetrahydrofuran; tpa, terephthalate.

* Corresponding author. Tel.: +351 218419207; fax: +351 218464455.
E-mail address: kirillov@ist.utl.pt

0010-8545/$ – see front matter
doi:10.1016/j.ccr.2011.01.023

of supramolecular networks and water clusters are described, and the selected properties and potential applications of hmt-containing coordination polymers as porous, magnetic or photoluminescent materials are highlighted.

1. Introduction

The crystal engineering of new coordination polymers (or metal-organic frameworks) is currently one of the sweeping research areas in coordination, supramolecular and materials chemistry, which also attracts significant attention due to the diverse practical applications of such compounds in fields ranging from molecular magnetism, adsorption science and gas storage to photoluminescence and catalysis [1,2]. Among the variety of organic ligands, different N-donors such as diamines and polypyridine derivatives have been broadly explored as building blocks and linkers for the construction of coordination networks [1–3]. Much research has also been focused on the development of new organic molecules with tunable properties toward their use in crystal engineering [1,2]. Surprisingly, the potential of some simple organic compounds that possess all the requirements to become common building blocks for the synthesis of coordination polymers has not been fully realized.

Hexamethylenetetramine (hmt), also known as hexamine or urotropine, can be considered as one such simple heterocyclic compound with a cagelike structure (Scheme 1) which, due to its inexpensiveness, commercial availability, high solubility in water and polar organic solvents, has found a broad variety of applications, ranging from the production of phenolic resins and solid fuel tablets to uses in organic synthesis, medicinal and materials chemistry [4,5]. With regard to coordination chemistry, hmt is a versatile ligand capable of adopting different coordination modes that span from the terminal monodentate to bridging bi-, tri- and tetradentate modes [5,6]. In addition, due to the good H-bond accepting behavior, hmt is very often trapped by metal-organic compounds forming various molecular adducts and supramolecular structures [6,7].

In fact, the current version of the Cambridge Structural Database (CSD) reveals more than 500 structurally characterized compounds comprising hmt [6], among them there are over 150 coordination polymers that possess diverse topologies and some interesting properties. The number of examples is, however, much inferior to that of polymeric networks built from other common N-donor ligands [3] such as 4,4′-bipyridine, 2,2′-bipyridine, ethylenediamine and pyrazine, for which ca. 2000, 1000, 650 and 450 hits, respectively, have been found in the CSD [6]. Moreover, about a half of hmt polymers are silver-based networks, which were classified and described in a comprehensive review by Chen et al. [5] and, in part, in prior studies by Zubieta et al. [8] and Carlucci et al. [9].

In contrast, the use of hmt as a simple and convenient linker (other common terms include spacer or connector) with a diamandoid-like geometry for the design of coordination polymers with other metals was explored to a lesser extent [6]. However, due to the sweeping development of crystal engineering the interest in hmt was regained in recent years, resulting in the synthesis of a good number of one- (1D), two- (2D) and there-dimensional (3D) hmt-driven coordination polymers bearing different metals [10–45]. Although these studies were primary focused on exploring rich structural diversity and attractive molecular aesthetics of hmt coordination polymers, the application of such compounds as functional materials still remains underdeveloped [14,17,18,25,26b]. This can be associated with synthetic serendipity and difficulties in controlling both the coordination number of hmt and the type of resulting metal-organic framework, as well as with somewhat reduced thermal and solvent stability of hmt polymers in comparison with the networks driven by aromatic N-donor building blocks.

Given the fact that this emerging area of research on coordination polymers of hmt has not yet been reviewed in spite of great potential for future developments, the main objectives of the present work consist in (i) providing an overview of the structural and topological types of hmt-driven coordination networks, (ii) classifying the most common ligands and synthetic strategies toward rational design of new compounds, and (iii) outlining the main properties of such metal-organic materials. The scope of this study does not cover numerous recent examples of silver coordination polymers with hmt [6,46], which can be the object of a separate review.

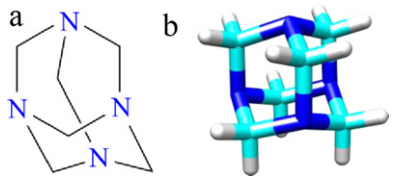

Scheme 1. Structural formula (a) and X-ray crystal structure (b) of hmt, $(CH_2)_6N_4$ [47].

2. General considerations

Within the structurally characterized compounds with hmt reported to date, 76 non-silver coordination polymers have been identified [6], wherein hmt possesses at least one coordination bond to a metal center. In the majority of these polymers (72 structures) hmt acts in a bridging mode, thus constituting a main group designated herein as hmt-driven coordination polymers. They are divided in sub-groups of 1D (**1**–**28**), 2D (**29**–**41**) and 3D (**42**–**72**) networks, which are summarized in Tables 1–3, respectively. The remaining four structures (compounds **73**–**76**) bear hmt as a terminal ligand and represent a tiny group of hmt-supported polymers (Table 4).

The first coordination polymers of hmt date back to 1981 when Pickardt reported the structures of compounds $[Cu_2(\mu_2\text{-ac})_4(\mu_2\text{-hmt})]_n$ (**19**) [48] and $[Cd_3I_4(\mu_2\text{-I})_2(\mu_2\text{-hmt})_2(H_2O)_2]_n{\cdot}2nH_2O$ (**39**) [49], which bear the dicopper tetraacetate and tricadmium hexaiodide cores, respectively. In the following two decades, this chemistry developped rather slowly, since only 12 and 15 structures were published in 1980s [50–57] and 1990s [58–68], respectively. However, the flourishing progress of crystal engineering yielded ca. 50 new structures in the past decade [10–45], nearly half of them was reported within the last three years. Bearing these features in mind and expecting even more pronounced growth of this research area in the near future, this review aims to consolidate the corresponding state-of-the-art knowledge and to attract attention toward the still limited use of hmt in the design of coordination polymers.

From the viewpoint of dimensionality, 1D (30 structures) and 3D (32 structures) networks are the most common, while 2D structures are found in only 14 compounds. In spite of having up to four available sites for the coordination, hmt typically adopts a μ_2-mode (51 structures), whereas μ_3- and μ_4-modes are much less common (13 and 6 examples, respectively). Although in the majority of cases

Table 1
One-dimensional hmt-driven coordination polymers.

Compound	Formula	M:hmt	1D chain type (topology)[a]	Extension via H-bonds[b]	Ref.
1	$[ZnCl_2(\mu_2\text{-hmt})]_n$	1:1	Linear (A1)		[52]
2	$[ZnBr_2(\mu_2\text{-hmt})]_n$	1:1	Linear (A1)		[52]
3	$[HgBr_2(\mu_2\text{-hmt})]_n$	1:1	Linear (A1)		[67]
4	$[HgI_2(\mu_2\text{-hmt})]_n$	1:1	Linear (A1)		[66]
5	$[CdBr(NCS)(\mu_2\text{-hmt})(H_2O)_2]_n\cdot n$MeOH	1:1	Zigzag (B1)	→3D	[12]
6	$[CdI(NCS)(\mu_2\text{-hmt})(H_2O)_2]_n\cdot 0.5n$MeOH	1:1	Zigzag (B1)	→3D	[12]
7	$[Zn(NCS)_2(\mu_2\text{-hmt})(H_2O)_2]_n$	1:1	Zigzag (B1)	→3D	[64]
8	$[Ni(NCS)_2(\mu_2\text{-hmt})(H_2O)_2]_n$	1:1	Zigzag (B1)	→2D	[27,43]
9	$[Hg(\mu_2\text{-NCS})_2(\mu_2\text{-hmt})]_n$	1:1	Double (D1)		[54]
10	$[Co(NCO)_2(\mu_2\text{-hmt})(H_2O)_2]_n$	1:1	Zigzag (B1)	→2D	[19]
11	$[Ni(NCO)_2(\mu_2\text{-hmt})(H_2O)_2]_n$	1:1	Zigzag (B1)	→2D	[19a]
12	$[Co(N_3)_2(\mu_2\text{-hmt})(H_2O)_2]_n$	1:1	Zigzag (B1)	→2D	[28]
13	$[Cd(NO_3)_2(\mu_2\text{-hmt})(H_2O)_2]_n$	1:1	Zigzag (B1)	→3D	[50]
14	$[Co(NO_3)_2(\mu_2\text{-hmt})(H_2O)_2]_n$	1:1	Zigzag (B1)	→3D	[15]
15	$[Cd(phac)_2(\mu_2\text{-hmt})(H_2O)]_n$	1:1	Zigzag (B1)	→2D	[10]
16	$[Cd(fba)_2(\mu_2\text{-hmt})(H_2O)]_n$	1:1	Zigzag (C1)	→3D	[13]
17	$[Cd(fba)_2(\mu_2\text{-hmt})(H_2O)_2]_n\cdot nH_2O$	1:1	Zigzag (B1)	→3D	[13]
18	$[Hg_2(\mu_2\text{-NCS})_4(\mu_2\text{-hmt})]_n$	2:1	Double (E1)		[53]
19	$[Cu_2(\mu_2\text{-ac})_4(\mu_2\text{-hmt})]_n$	2:1	Zigzag (B1)		[48]
20	$[Ni_2(\mu_2\text{-ac})_4(\mu_2\text{-hmt})]_n$	2:1	Zigzag (B1)		[38]
21	$[Cu_2(\mu_2\text{-phca})_4(\mu_2\text{-hmt})]_n\cdot 0.75nH_2O$	2:1	Zigzag (B1)		[11]
22	$[Cu_2(\mu_2\text{-adca})_4(\mu_2\text{-hmt})]_n$	2:1	Zigzag (B1)		[11]
23	$[Co_2Cu_2(CO)_8(\mu_2\text{-hmt})_2]_n\cdot n$THF	2:1	Zigzag (B1)		[61]
24	$[Cd_2(\mu_2\text{-SCN})_2(SCN)_2(\mu_2\text{-hmt})(hmt)_2(H_2O)_2]_n\cdot nH_2O$	2:3	Zigzag (B1)	→2D	[12]
25	$[Cd_3(\mu_2\text{-NCS})_6(\mu_2\text{-hmt})_2(H_2O)_2]_n$	3:2	Triple (F1)	→2D	[36]
26	$[Cd_3(\mu_2\text{-NCSe})_6(\mu_2\text{-hmt})_2(H_2O)_2]_n$	3:2	Triple (F1)	→2D	[23]
27	$[Mn_3(\mu_3\text{-O})(\mu_2\text{-ibut})_6(\mu_2\text{-hmt})(hmt)]_n\cdot n$EtOH	3:2	Linear (A1)		[21]
28	$[Cu_4(\mu_2\text{-mal})_4(\mu_4\text{-hmt})(H_2O)_4]_n\cdot 3nH_2O$	4:1	Quadruple (G1)	→3D	[34]

[a] Topologies are those of Scheme 2.
[b] Conventional H-bonds and short contacts are taken into consideration.

hmt exhibits only one type of coordination, some rare examples with mixed coordination modes of hmt have also been reported, namely 1D $[Mn_3(\mu_3\text{-O})(\mu_2\text{-ibut})_6(\mu_2\text{-hmt})(hmt)]_n\cdot n$EtOH (**27**) [21], 2D $[Cu_2(\mu_2\text{-prop})_4(\mu_4\text{-hmt})(\mu_3\text{-hmt})_2]_n$ (**34**) [41], and 3D $[Na_3(\mu_2\text{-}H_2O)_5\{\mu_3\text{-Fe}(CN)_6\}(\mu_2\text{-hmt})(hmt)]_n$ (**56**) [56], $[Cd_4(\mu_2\text{-tar})_4(\mu_4\text{-hmt})(\mu_2\text{-hmt})_2(H_2O)_4]_n\cdot 8nH_2O$ (**69**) [69] and $\{Na[Cd_4(\mu_2\text{-Cl})(\mu_2\text{-dpa})_4(\mu_2\text{-hmt})(hmt)(H_2O)_6]\cdot(H_2O)_4\}_n$ (**72**) [25] coordination polymers. Besides, most of the hmt-driven polymers are neutral, except the three cationic networks $[Cd(\mu_3\text{-tcm})(\mu_2\text{-hmt})(H_2O)]_n(tcm)_n$ (**42**) [68], $[\{Cd_{34}(\mu_4\text{-hmt})_{17}(H_2O)_{102}\}_n(Cl)_{68n}\cdot 46nH_2O\cdot 68n$DMF (**57**) [29] and $[Cd_3(\mu_2\text{-male})_2(\mu_3\text{-hmt})_2(H_2O)_8]_n(SO_4)_n\cdot 2nH_2O$ (**67**) [30]. A unique anionic network $\{[hmtH]_2[Pb_3I_2(\mu_3\text{-I})_2(\mu_2\text{-I})_4(hmt)_2]\}_n$ (**74**) [57] was, however, observed within one of the hmt-supported polymers [57,58,62,70].

As mentioned above, in contrast to rich family of Ag-hmt coordination polymers [5,6,46], the hmt containing networks based on other metals are less common [6], with cadmium (31 structures) and copper (15 structures) representing the most numerous examples. The occurrence of compounds with other metals follows the trend: Hg (7) > Co (6) > Zn (5) > Mn (3), Ni (3) > Na (1), Pb (1) (figures in brackets correspond to the number of known homometallic coordination polymers of hmt). Besides, five heterometallic Cu/Co (**23**) [61], Na/Fe (**56**) [56], Ca/Fe (**64**) [55], Cd/Na (**72**) [25] and Co/K (**76**) [70] networks have been identified, but all possess hmt moieties coordinated to only one metal (first in the above pairs). Although the observed metal-to-hmt molar ratios (M:hmt) span from 2:3 to 5:1, the most common ones are 1:1 (22 structures, mainly 1D polymers), 2:1 (22 structures, mainly 3D polymers), 3:2 (12 structures, mainly 2D polymers) and 3:1 (9 structures, mainly 3D polymers).

The present review shows that hmt-driven coordination polymers feature a high diversity of structural motifs and topologies that range from linear, zigzag, double, triple and quadruple 1D chains (Table 1) to rectangular grids, flat and undulating 2D layers (Table 2), as well as to layer-pillared, octahedral, zeolite-like, honeycomb-like and other complex 3D nets (Table 3), in which the versatile hexamethylenetetramine plays a number of roles acting as a linker or spacer, pillar or connector, stabilizer and/or supporting ligand. Hence, more detailed descriptions of topologies and structural features of hmt-driven coordination polymers are given below. The structural ball-and-stick representations of selected examples (Figs. 1–9) were designed with Mercury software [71] using CIF files from the CSD [6].

3. Hmt-driven coordination polymers

3.1. One-dimensional chains

The analysis of 1D coordination polymers (compounds **1**–**28**, Table 1) led to the identification of seven different topological motifs A1–G1, their simplified representation is given in Scheme 2. The linear (type A1) and zigzag (type B1) chains represent the most common motifs observed in 5 (**1**–**4**, **27**) and 17 (**5**–**8**, **10**–**14**, **17**, **19**–**24**) structures, respectively. Other identified motifs are limited to particular compounds, namely a tooth-shaped zigzag chain (C1) in $[Cd(fba)_2(\mu_2\text{-hmt})(H_2O)]_n$ (**16**) [13], a double chain (D1) in $[Hg(\mu_2\text{-NCS})_2(\mu_2\text{-hmt})]_n$ (**9**) [54], a ladder (E1) in $[Hg_2(\mu_2\text{-NCS})_4(\mu_2\text{-hmt})]_n$ (**18**) [53], a 3-leg ladder (F1) in $[Cd_3(\mu_2\text{-NCS})_6(\mu_2\text{-hmt})_2(H_2O)_2]_n$ (**25**) [36] and $[Cd_3(\mu_2\text{-NCSe})_6(\mu_2\text{-hmt})_2(H_2O)_2]_n$ (**26**) [23], and a quadruple cyclic chain (G1) in $[Cu_4(\mu_2\text{-mal})_4(\mu_4\text{-hmt})(H_2O)_4]_n\cdot 3nH_2O$ (**28**) [34]. Interestingly, almost all 1D networks feature a μ_2-coordination mode of hmt, the unique exception concerns the compound **28** wherein hmt acts as a μ_4-linker. The A1–C1 motifs can be classified as self-sufficient involving only hmt as a linker, while the construction of the D1–G1 motifs requires the use of additional bridging ligands (Scheme 2).

Linear chain motifs (A1) were observed in simple polymers **1**–**4** [52,66,67] with a similar $[M(X)_2(\mu_2\text{-hmt})]_n$ (M = Zn or Hg; X = halide) general formula (for typical example, see Fig. 1a). Another interesting compound $[Mn_3(\mu_3\text{-O})(\mu_2\text{-ibut})_6(\mu_2\text{-hmt})(hmt)]_n\cdot n$EtOH (**27**) is constructed from trinuclear $[Mn_3(\mu_3\text{-}$

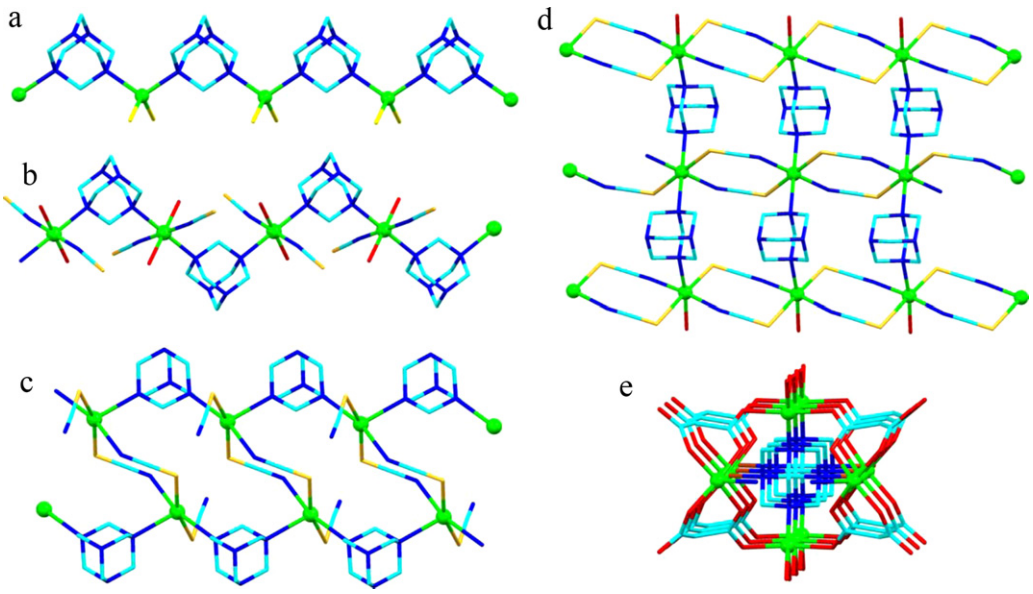

Fig. 1. Structural fragments of **1** (a) [52], **8** (b) [43], **9** (c) [54], **25** (d) [36] and **28** (e) [34] showing linear (a), zigzag (b), double (c), 3-leg ladder (d) and quadruple cyclic (e) 1D chains. H atoms and solvent molecules are omitted for clarity. Hereinafter typical color codes are the following: metal atoms (green balls), C (cyan), N (blue), O (red), halide (yellow), S (orange).

O)(μ_2-ibut)$_6$] cluster nodes bridged by μ_2-hmt in a linear fashion [21]. A noteworthy feature of this Mn(II)/Mn(III) polymer consists in the mixed-valence of its metal atoms, which is not observed in any other coordination polymer of hmt.

Within the most populated family of zigzag chain polymers (for typical example, see Fig. 1b), two main groups of compounds can be identified based on the metal-to-hmt molar ratio (M:hmt). The first group with the M:hmt of 1:1 includes compounds **5**–**8**, **10**–**15** and **17**. All of them have quite similar general formulae and are composed of a metal atom (Co, Ni, Zn or Cd), two coordinated anions (Br, I, NCS, NCO, N_3, NO_3, phac and fba, or their combination), one or two coordinated H_2O molecules and one μ_2-hmt moiety. Some of these compounds are isostructural (e.g. **5** and **6**, **10**–**12**, **13** and **14**). The second group of zigzag polymers consists of compounds **19**–**23** that possess the M:hmt of 2:1, owing to the presence of bimetallic paddle-wheel [$M_2(L)_4$] (M = Cu or

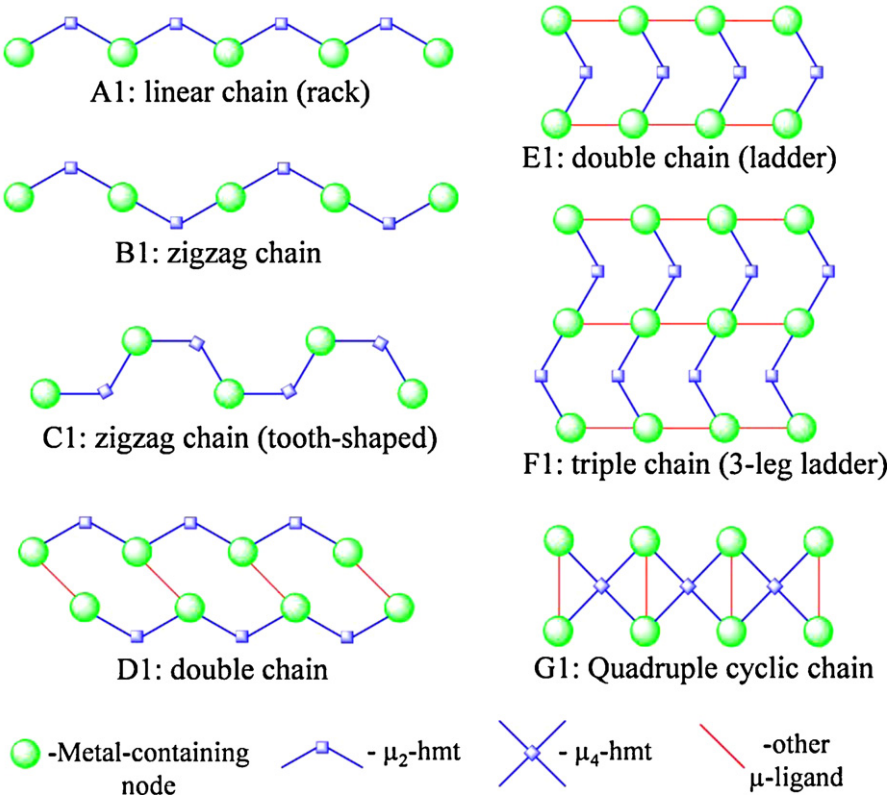

Scheme 2. Simplified representation of diverse structural motifs (A1–G1) identified in the crystal structures of 1D coordination polymers **1**–**28** (see also Table 1). Metal containing nodes (green balls) can be composed of up to four metal centers, while other bridging ligands (red sticks) can provide multiple linkages between the neighboring nodes.

Ni; L = μ_2-carboxylate) or tetrametallic carbonyl $[M_4(CO)_8]$ (M = Cu and Co) nodes. A compound $[Co_2Cu_2(CO)_8(\mu_2\text{-hmt})_2]_n{\cdot}n$THF (**23**) [61] also represents the unique example of a heterometallic 1D hmt-driven coordination polymer, as well as a rare case of the organometallic coordination network composed of cluster nodes. Although **23** was reported almost two decades ago [61], such a type of carbonyl chemistry with hmt has not received further development.

Two different types of double chain motifs (D1 and E1, Scheme 2) were observed in the Hg(II) polymers **9** [54] and **18** [53] which, in addition to μ_2-hmt, also comprise μ_2-NCS moieties. In **9**, these thiocyanate groups provide a double linkage of adjacent Hg-hmt racks (Fig. 1c), whereas in **18** the same role is played by hmt molecules that "sew" the two loop-like ~Hg(μ_2-NCS)~ linear chains forming a ladder structure. A similar feature is observed in the isostructural cadmium polymers **25** [36] and **26** [23] in which μ_2-hmt moieties act as connectors between three ~Cd(μ_2-NCS)~ or ~Cd(μ_2-NCSe)~ chains, respectively, thus generating a 3-leg ladder structure (Fig. 1d).

The quadruple cyclic chain (G1, Scheme 2) was identified in the unique 1D polymer **28** [34] with a μ_4-mode of hmt and the M:hmt ratio of 4:1. Such peculiar topology is made possible owing to the formation of cyclic tetracopper(II) malonate entities that are assembled by tetradentate μ_4-hmt linkers (Fig. 1e).

An important feature of many hmt-driven 1D polymers consists in the further extension of their one-dimensional coordination chains, via multiple hydrogen bonds and/or short contacts, to form either 2D (in **8**, **10**–**12**, **15**, **24**–**26**) or 3D (in **5**–**7**, **13**, **14**, **16**, **17**, **28**) supramolecular structures (Table 1). Their formation is typically driven by strong H-bonds in those compounds that bear coordinated and/or crystallization water molecules. Besides, the recognized H-bond accepting behavior of hmt facilitates such a type of interactions.

3.2. Two-dimensional layers and grids

Although 1D chains were reported for different metals (Cd, Hg, Cu, Zn, Co, Ni, Mn), the group of hmt-driven 2D coordination polymers **29**–**41** (Table 2) is still limited to compounds of cadmium and copper (8 and 5 structures, respectively). With regard to a coordination mode of hmt, eight polymers bear μ_2-hmt, four compounds comprise μ_3-hmt, and one unique structure (**34**) features the presence of both μ_3- and μ_4-hmt linkers. The six different M:hmt ratios were observed, but the most common ones are 3:2 and 2:1. In general, the 2D polymers are neutral and composed of metal atoms coordination spheres of which are filled by anionic ligands, water molecules (optional) and bridging hmt moieties. The anionic ligands can be both simple (Cl, Br, I, CN, NCS, acetate, propionate) and more complex (e.g. dpa, pbpd, tcm, opbh) which, however, typically act in a bridging mode. Hence, the construction of the majority of 2D networks is not solely based on hmt, but also involves other connecting species. The simplified topological representations of 2D motifs observed in **29**–**41** are given in Schemes 3 and 4.

Taking into consideration only the metal–hmt interactions, two types of topologies were identified (Scheme 3), namely the honeycomb-like hexagons in $[Cd_3Br_6(\mu_3\text{-hmt})_2(H_2O)_5]_n{\cdot}n$(hmt)·6$nH_2$O (**38**) [12], $[Cd_3(ac)_6(\mu_3\text{-hmt})_2(H_2O)_3]_n{\cdot}6nH_2O$ (**40**) [10] and $[Cu_3(\mu_2\text{-pbpd})_3(\mu_3\text{-hmt})]_n$ (**35**) [24], and the periodically tiled pentagons in $[Cu_2(\mu_2\text{-prop})_4(\mu_4\text{-hmt})(\mu_3\text{-hmt})_2]_n$ (**34**) [41].

Compounds **38** and **40** feature the almost regular hexagon rings that are constructed from six μ_3-hmt linkers and six monocadmium nodes (for typical example, see Fig. 2a). Interestingly, three different types of the latter (i.e. a pair of $[CdBr(H_2O)_3]^+$, $[CdBr_2(H_2O)_2]$ and $[CdBr_3]^-$) are present in **38** [12], while only one type of the node, $[Cd(ac)_2(H_2O)]$, is observed in **40** [10]. The copper(II) polymer **35** [24] is built from the fused chiral hexagons $[(Cu_2)_6(hmt)_6(pbpd)_{12}]$ that possess a very distorted topology. The infinite 2D layers of **38**, **40** and **35** are undulating and thus exhibit the bent honeycomb-like topologies.

As mentioned above, compound **34** reported by Zaworotko et al. [41] features a unique combination of μ_3- and μ_4-hmt moieties, thus presumably constituting a driving force toward the formation of the unprecedented $5,^3_4$-net topology via periodic tiling of nonregular pentagons (Fig. 2b). Each pentagon is constructed from five propeller-like $[Cu_2(\mu_2\text{-prop})_4]$ clusters, two μ_4- and three μ_3-hmt moieties.

Within the 2D networks **29**–**33**, **36**, **37**, **40** and **41** (Table 2) constructed from hmt and other bridging ligands, eight different

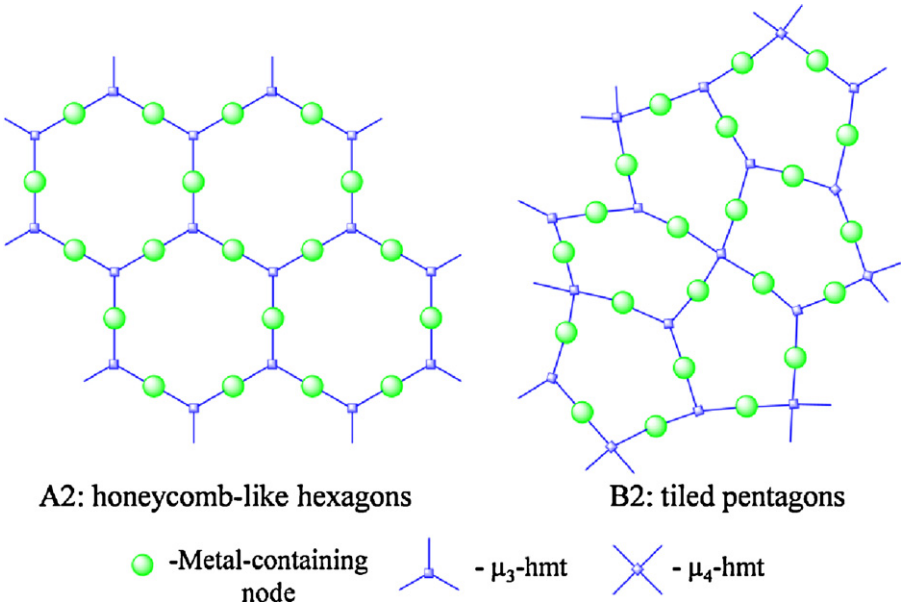

Scheme 3. Simplified representation of 2D topologies formed exclusively via the metal–hmt interactions in the crystal structures of coordination polymers **40**, **38** and **35** (A2), or **34** (B2). Metal containing nodes (green balls) can be composed of up to two metal centers.

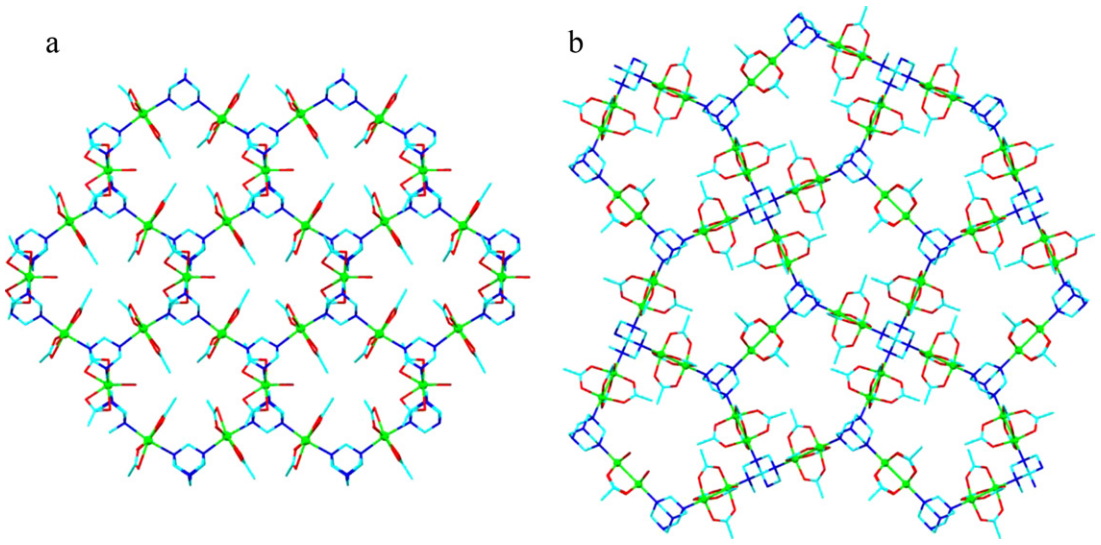

Fig. 2. Structural fragments of **40** (a) [10] and **34** (b) [41] showing the formation of honeycomb-like hexagons (a) and tiled pentagons (b), if viewed along the *c* axis. H atoms, solvent molecules and Me groups of prop ligands (in **34**) are omitted for clarity.

topologies were identified (Scheme 4, C2–J2). These include rectangular grids (C2, D2), flat (E2, G2) and undulating (F2, H2, I2, J2) layers, which can be rationalized as a collection of repeating cyclic motifs $M_x(hmt)_y(L)_z$ composed of metal nodes (M; $x = 3–8$), hmt linkers ($y = 1–5$) and other bridging ligands (L; $z = 2–8$). The C2–D2 topologies are defined by a single type of such cyclic motifs, while the H2–J2 topologies are formed via the combination of two types of cyclic motifs (Scheme 4, Table 2).

Alternatively, some topologies can also be described as different hmt-driven 1D chains sewed into 2D networks via other bridging ligands, or vice versa. For example, $[Cu(\mu_2\text{-tcm})(\mu_2\text{-hmt})]_n$ (**29**) [44] and $[Cd(\mu_2\text{-dca})_2(\mu_2\text{-hmt})]_n$ (**30**) [23] possess linear or zigzag metal–hmt chains interconnected by μ_2-tcm or μ_2-dca ligands, respectively, to form rectangular grids (Fig. 3a). A noteworthy feature of **29** consists in the interdigitation of adjacent grids [44]. In other cases, μ_2-hmt acts as a connector between the neighboring 1D zigzag chains, giving rise to 2D layers in $[Cd_2(\mu_2\text{-NCS})_4(\mu_2\text{-hmt})(H_2O)_2]_n{\cdot}nH_2O$ (**32**) [16] (Fig. 3b), $[Cu_2(\mu_2\text{-opbh})_2(\mu_2\text{-hmt})]_n$ (**33**) [31] and $[Cd_3Br_2(\mu_2\text{-Br})_4(\mu_2\text{-hmt})_2(H_2O)_4]_n{\cdot}2nH_2O$ (**37**) [45].

An interesting 2D network (H2, Scheme 4) is formed in $[Cu_3(\mu_2\text{-CN})_3(\mu_2\text{-hmt})_2]_n$ (**36**) [59], wherein almost regular $Cu_6(hmt)_2(CN)_4$ hexagons and twisted-square tetracopper $Cu_4(hmt)_2(CN)_2$ rings are periodically tiled to furnish an undulating layer (Fig. 3c). Two cyclic motifs, $Cd_4(hmt)_2(Cl)_2$ and $Cd_3(hmt)(Cl)_2$, are also present in $[Cd_4Cl_4(\mu_2\text{-Cl})_4(\mu_3\text{-hmt})_2(H_2O)_6]_n{\cdot}4nH_2O$ (**31**) [51], in which the μ_3-hmt moieties provide a triple linkage of neighboring wave-like cadmium chloride chains (Fig. 3d).

As in the case of 1D polymers (Table 1), all hmt-driven 2D networks that possess coordinated and crystallization water molecules (i.e. **31**, **32**, **37**–**41**) are extended to 3D supramolecular structures via numerous H-bonding interactions. The analysis of these interactions led to the identification of various water associates (see section 6.1) trapped within the host 2D metal-organic matrices

Table 2
Two-dimensional hmt-driven coordination polymers.

Compound	Formula	M:hmt	2D network type (topology)[a]	Repeating cyclic motifs[b]	Extension via H-bonds[c]	Ref.
29	$[Cu(\mu_2\text{-tcm})(\mu_2\text{-hmt})]_n$	1:1	Puckered rectangular grid (C2)	$Cu_4(hmt)_2(tcm)_2$		[44]
30	$[Cd(\mu_2\text{-dca})_2(\mu_2\text{-hmt})]_n$	1:1	Rectangular grid (D2)	$Cu_4(hmt)_2(dca)_2$		[23]
31	$[Cd_4Cl_4(\mu_2\text{-Cl})_4(\mu_3\text{-hmt})_2(H_2O)_6]_n{\cdot}4nH_2O$	2:1	Undulating layer (J2)	$Cd_4(hmt)_2(Cl)_2 + Cd_3(hmt)(Cl)_2$	→3D	[51]
32	$[Cd_2(\mu_2\text{-NCS})_4(\mu_2\text{-hmt})(H_2O)_2]_n{\cdot}nH_2O$	2:1	Flat layer (E2)	$Cd_6(hmt)_2(NCS)_8$	→3D	[16]
33	$[Cu_2(\mu_2\text{-opbh})_2(\mu_2\text{-hmt})]_n$	2:1	Flat layer (E2)	$Cu_6(hmt)_2(opbh)_6$		[31]
34	$[Cu_2(\mu_2\text{-prop})_4(\mu_4\text{-hmt})(\mu_3\text{-hmt})_2]_n$	2:3	Net from tiled pentagons (B2)	$(Cu_2)_5(hmt)_5$		[41]
35	$[Cu_3(\mu_2\text{-pbpd})_3(\mu_3\text{-hmt})]_n$	3:1	Distorted honeycomb-like layer (A2)	$(Cu_2)_6(hmt)_6$		[24]
36	$[Cu_3(\mu_2\text{-CN})_3(\mu_2\text{-hmt})_2]_n$	3:2	Undulating layer (H2)	$Cu_6(hmt)_2(CN)_4 + Cu_4(hmt)_2(CN)_2$		[18,59]
37	$[Cd_3Br_2(\mu_2\text{-Br})_4(\mu_2\text{-hmt})_2(H_2O)_4]_n{\cdot}2nH_2O$	3:2	Undulating layer (F2)	$Cd_8(hmt)_4(Br)_8$	→3D	[45]
38	$[Cd_3Br_6(\mu_3\text{-hmt})_2(H_2O)_5]_n{\cdot}n(hmt){\cdot}6nH_2O$	3:2	Bent honeycomb-like layer (A2)	$Cd_6(htm)_6$	→3D	[12]
39	$[Cd_3I_4(\mu_2\text{-I})_2(\mu_2\text{-hmt})_2(H_2O)_2]_n{\cdot}2nH_2O$	3:2	Flat layer (G2)	$Cd_8(hmt)_4(I)_4$	→3D	[49]
40	$[Cd_3(ac)_6(\mu_3\text{-hmt})_2(H_2O)_3]_n{\cdot}6nH_2O$	3:2	Bent honeycomb-like layer (A2)	$Cd_6(hmt)_6$	→3D	[10]
41	$[Cd_4(\mu_2\text{-dpa})_4(\mu_2\text{-hmt})_3(H_2O)_5]_n{\cdot}10nH_2O$	4:3	Flat layer (I2)	$Cd_8(hmt)_5(dpa)_4 + Cd_4(hmt)(dpa)_3$	→3D	[25]

[a] Topologies are those of Schemes 3 and 4.
[b] All ligands within these motifs are bridging (symbol μ is omitted for simplicity).
[c] Conventional H-bonds and short contacts are taken into consideration.

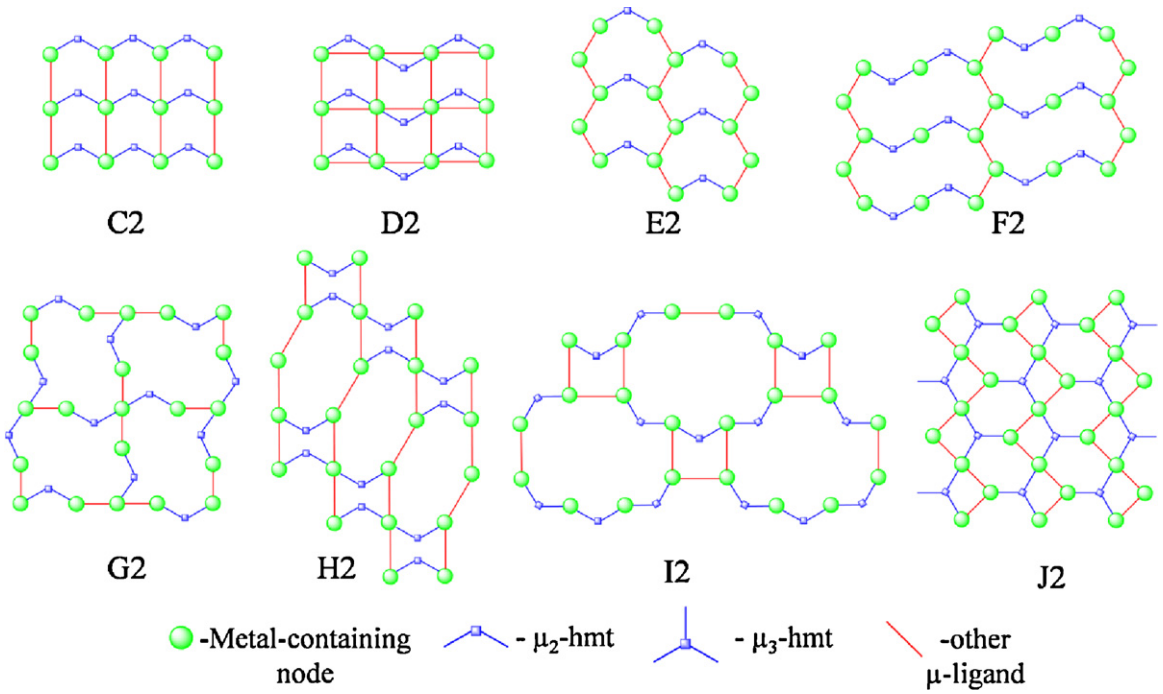

Scheme 4. Simplified representation of 2D topologies, formed via interactions involving hmt and other bridging ligands, in the crystal structures of coordination polymers: **29** (C2), **30** (D2), **32** and **33** (E2), **37** (F2), **39** (G2), **36** (H2), **41** (I2) and **31** (J2). Other bridging ligands (red sticks) can provide multiple linkages between the neighboring nodes.

of coordination polymers. Besides, the structure of **38** also bears the uncoordinated guest molecules of hmt, each of them acts as an acceptor of four H-bonds, thus providing a 3D supramolecular network [12].

3.3. *Three-dimensional frameworks*

The 3D networks **42**–**72** (Table 3) constitute the most interesting and diverse group of hmt-driven coordination polymers, namely

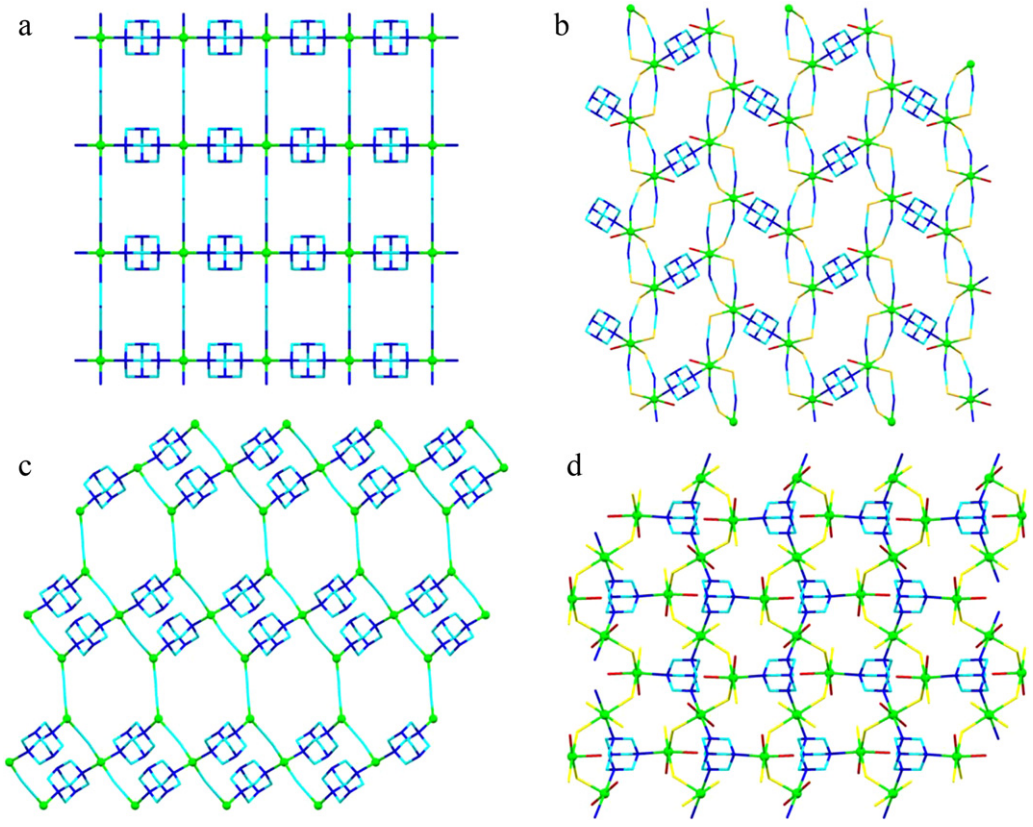

Fig. 3. Selected examples of topologically different hmt-driven 2D networks in the crystal structures of **29** (a) [44], **32** (b) [16], **36** (c) [59] and **31** (d) [51]; views along the *b* (a, c, d) or *c* (b) axis. H atoms and solvent molecules are omitted for clarity.

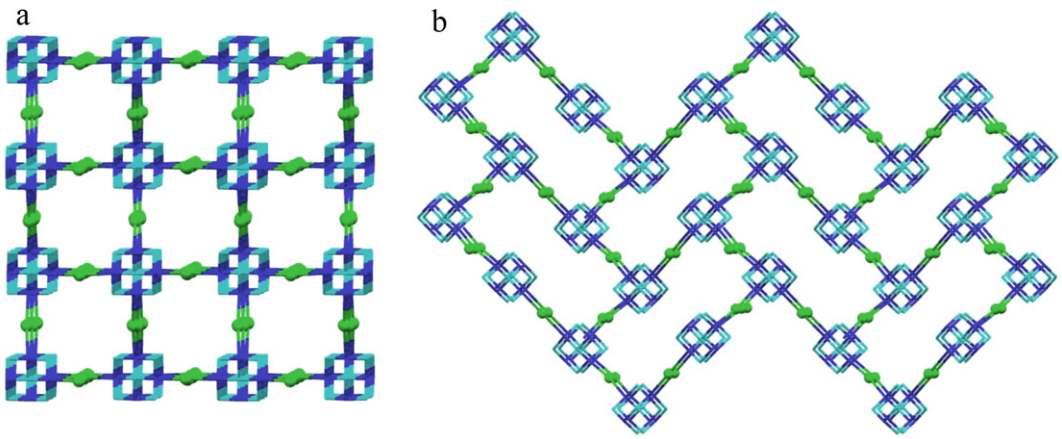

Fig. 4. Simplified structural fragments of **47** (a) [22] and **66** (b) [63] showing the formation of octahedral (a) and "parquet floor" (b) 3D skeletons formed exclusively via metal–hmt interactions (views along the *c* and *a* axes, respectively). H atoms, Cl, MeOH and NCS ligands are omitted for clarity.

Table 3
Three-dimensional hmt-driven coordination polymers.

Compound	Formula	M:hmt	Hmt motif or function (sub-group)	Overall 3D network type	Ref.
42	$[Cd(\mu_3\text{-tcm})(\mu_2\text{-hmt})(H_2O)]_n(tcm)_n$	1:1	1D Cd-hmt zigzag chains (B3)	Octahedral rutile-like	[68]
43	$[Cd_2(\mu_3\text{-pdc})_2(\mu_2\text{-hmt})_2(H_2O)_2]_n\cdot 2nDMF\cdot 2nH_2O$	1:1	Pillar between 2D Cd-pdc layers (C3)	Layer-pillared	[17]
44	$[Cd_2(\mu_2\text{-tpa})_2(\mu_2\text{-hmt})_2(H_2O)_3]_n\cdot 3nH_2O$	1:1	1D Cd-hmt zigzag chains (B3)	Layered tooth-shaped[a]	[36]
45	$[Hg_2Br_2(\mu_2\text{-Br})_2(\mu_2\text{-hmt})]_n$	2:1	Linker between 1D Hg-Br motifs (C3)	Zeolite-like	[42]
46	$[Hg_2(\mu_2\text{-Cl})_4(\mu_4\text{-hmt})]_n$	2:1	Pillar between 1D Hg-Cl motifs (C3)	Honeycomb-like	[37]
47	$[Cd_2Cl_2(\mu_2\text{-Cl})_2(\mu_4\text{-hmt})(MeOH)_2]_n$	2:1	3D Cd-hmt octahedral net (A3)	Octahedral	[22]
48	$[Co_2(\mu_2\text{-}N_3)_4(\mu_3\text{-hmt})(H_2O)]_n$	2:1	Stabilizer of 3D Co-N_3 network (D3)	Complex net with rutile or pyrite topology	[14]
49	$[Cu_2(\mu_3\text{-mal})_2(\mu_2\text{-hmt})(H_2O)_2]_n$	2:1	Pillar between 2D Cu-mal layers (C3)	Layer-pillared	[33]
50	$[Co_2(\mu_3\text{-mal})_2(\mu_2\text{-hmt})(H_2O)_2]_n$	2:1	Pillar between 2D Co-mal layers (C3)	Layer-pillared	[34]
51	$[Zn_2(\mu_3\text{-mal})_2(\mu_2\text{-hmt})(H_2O)_2]_n$	2:1	Pillar between 2D Zn-mal layers (C3)	Layer-pillared	[33a]
52	$[Cd_2(\mu_3\text{-mal})_2(\mu_2\text{-hmt})(H_2O)_2]_n$	2:1	Pillar between 2D Cd-mal layers (C3)	Layer-pillared	[40]
53	$[Mn_2(\mu_3\text{-mal})_2(\mu_2\text{-hmt})(H_2O)_2]_n$	2:1	Pillar between 2D Mn-mal layers (C3)	Layer-pillared	[35,33b]
54	$[Cu_2(\mu_4\text{-pma})(\mu_2\text{-hmt})(H_2O)_4]_n\cdot 8nH_2O$	2:1	Pillar between 2D Cu-pma grids (C3)	Grid-pillared	[39]
55	$[Mn_2(\mu_4\text{-pdc})_2(\mu_2\text{-hmt})(H_2O)_2]_n$	2:1	Pillar between 2D Mn-pdc layers (C3)	Layer-pillared	[17]
56	$[Na_3(\mu_2\text{-}H_2O)_5\{\mu_3\text{-}Fe(CN)_6\}(\mu_2\text{-hmt})(hmt)]_n$	2:1	Linker between 2D Na/Fe grids (C3)	Octahedral	[56]
57	$[\{Cd_{34}(\mu_4\text{-hmt})_{17}(H_2O)_{102}\}_n(Cl)_{68n}\cdot 46nH_2O\cdot 68n$DMF	2:1	3D Cd-hmt zeolite-like net (A3)	Zeolite-like	[29]
58	$[Na_3(\mu_3\text{-}NO_3)_3(\mu_3\text{-hmt})]_n$	3:1	Stabilizer of 3D Na-NO_3 network (D3)	Complex net	[20]
59	$[Cd_3(\mu_2\text{-CN})_6(\mu_4\text{-hmt})]_n$	3:1	Stabilizer of 3D Cd-CN network (D3)	Honeycomb-like	[60]
60	$[Cd_3(\mu_2\text{-CN})_5(\mu_3\text{-OH})(\mu_3\text{-hmt})]_n$	3:1	Stabilizer of 3D Cd-CN network (D3)	Honeycomb-like	[60]
61	$[Cd_3(\mu_6\text{-ctc})_2(\mu_2\text{-hmt})(DMF)(EtOH)(H_2O)]_n\cdot 3nH_2O$	3:1	Pillar between 2D Cd-ctc layers (C3)	Wave-like layer-pillared	[32]
62	$[Cu_3(\mu_2\text{-pbhd})_3(\mu_3\text{-hmt})]_n$	3:1	Linker between 0D Cu-pbhd units (C3)	Complex chiral net	[26a]
63	$[Cu_3(\mu_2\text{-bpbpd})_3(\mu_3\text{-hmt})]_n\cdot 22.5n$THF	3:1	Linker between 0D Cu-bpbpd units (C3)	Complex chiral net	[26b]
64	$[Ca_2\{\mu_6\text{-}Fe(CN)_6\}(\mu_2\text{-hmt})(\mu_2\text{-}H_2O)_2]_n\cdot 2nH_2O$	3:1	Stabilizer of 3D Ca/Fe network (D3)	Distorted octahedral	[55]
65	$[Cd_3(\mu_2\text{-CN})_6(\mu_3\text{-hmt})_2]_n$	3:2	2D Cd-hmt "brick wall" layers (B3)	Complex net	[65]
66	$[Hg_3(\mu_2\text{-Cl})_4(\mu_2\text{-NCS})_2(\mu_3\text{-hmt})_2]_n$	3:2	3D Hg-hmt "parquet floor" net (A3)	Complex net	[63]
67	$[Cd_3(\mu_2\text{-male})_2(\mu_3\text{-hmt})_2(H_2O)_8]_n(SO_4)_n\cdot 2nH_2O$	3:2	2D Cd-hmt honeycomb-like layers (B3)	Honeycomb-like	[30]
68	$[Zn_4(\mu_3\text{-pdc})_4(\mu_2\text{-hmt})(H_2O)_6]_n\cdot 4nDMA\cdot 5nH_2O$	4:1	Pillar between 2D Zn-pdc layers (C3)	Layer-pillared	[17]
69	$[Cd_4(\mu_2\text{-tar})_4(\mu_4\text{-hmt})(\mu_2\text{-hmt})_2(H_2O)_4]_n\cdot 8nH_2O$	4:3	2D Cd-hmt square-grid layers (B3)	Octahedral	[69]
70	$[Cu_5(\mu_3\text{-CN})_4(\mu_2\text{-CN})(\mu_4\text{-hmt})]_n$	5:1	Stabilizer of 3D Cu-CN network (D3)	Complex net	[18]
71	$[Cu_5(\mu_3\text{-CN})_4(\mu_2\text{-CN})(\mu_3\text{-hmt})_2]_n$	5:2	Stabilizer of 3D Cu-CN network (D3)	Complex net	[18]
72	$\{Na[Cd_4(\mu_2\text{-Cl})(\mu_2\text{-dpa})_4(\mu_2\text{-hmt})(hmt)(H_2O)_6]\cdot(H_2O)_4\}_n$	5:2	1D Cd-hmt zigzag chains (B3)	Complex net	[25]

[a] Although this compound was reported [36] as a 3D polymer, it apparently features a 2D layered coordination network which, however, is extended via H-bonds to a 3D supramolecular structure.

Table 4
Hmt-supported coordination polymers.

Compound	Formula	M:hmt	Overall network type	Ref.
73	$[Cd(\mu_2\text{-NCS})_2(hmt)(H_2O)]_n\cdot nH_2O$	1:1	1D Cd-NCS linear chain	[36,62]
74	$\{[hmtH]_2[Pb_3I_2(\mu_3\text{-I})_2(\mu_2\text{-I})_4(hmt)_2]\}_n$	3:2	1D Pb-I helical chain	[57]
75	$[Co(\mu_3\text{-dtb})(hmt)]_n$	1:1	2D Co-dtb flat layer	[58]
76	$[CoK_2(\mu_6\text{-nta})(hmt)(\mu_2\text{-}H_2O)_3]_n\cdot n NO_3$	3:1	3D honeycomb-like net	[70]

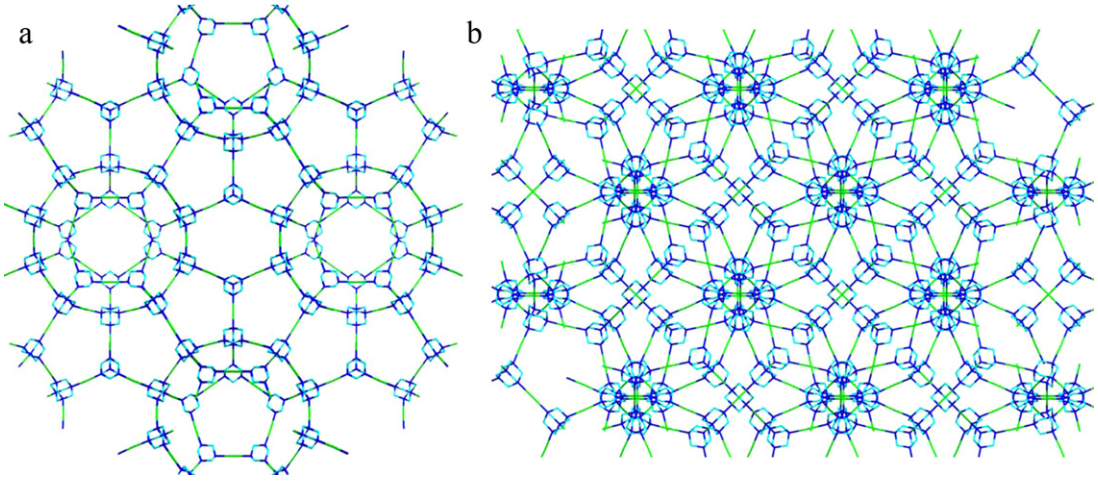

Fig. 5. Simplified structural fragments of **57** [29] (arbitrary views) showing the unique open 3D framework with the zeolite MTN topology. H atoms and H_2O molecules are omitted for clarity. For simplicity, Cd atoms are shown as green sticks.

due to the variety of observed topologies and the involvement of different types of (i) metals (i.e. homometallic Cd, Cu, Hg, Co, Mn, Zn and Na, and heterometallic Na/Fe, Ca/Fe and Cd/Na networks), (ii) bridging ligands, and (iii) coordination modes of hmt and the metal-to-hmt molar ratios. Taking into consideration the different roles played by hmt in the construction of 3D metal-organic frameworks, compounds **42**–**72** (Table 3) can be divided in the following sub-groups: (A3) 3D networks built via metal–hmt interactions, (B3) 1D or 2D metal–hmt motifs extended to a third dimension by means of other bridging ligands, (C3) 3D networks wherein hmt acts as a pillar (or linker) between 0D, 1D or 2D metal-organic motifs, and (D3) 3D nets constructed from other ligands that are only reinforced by bridging hmt moieties (hmt acts as a stabilizer).

Although the sub-group A3 includes only three compounds, $[Cd_2Cl_2(\mu_2\text{-}Cl)_2(\mu_4\text{-hmt})(MeOH)_2]_n$ (**47**) [22], $[\{Cd_{34}(\mu_4\text{-hmt})_{17}(H_2O)_{102}\}_n(Cl)_{68n}\cdot 46nH_2O\cdot 68n$DMF (**57**) [29] and $[Hg_3(\mu_2\text{-}Cl)_4(\mu_2\text{-}NCS)_2(\mu_3\text{-hmt})_2]_n$ (**66**) [63], they represent the most notable examples of 3D hmt-driven frameworks constructed via metal–hmt interactions. Hence, compound **47** possesses an octahedral net structure composed of cross-linking ~$CdCl_2$-μ_4-hmt-$CdCl_2$-μ_4-hmt~ motifs that form square "windows"

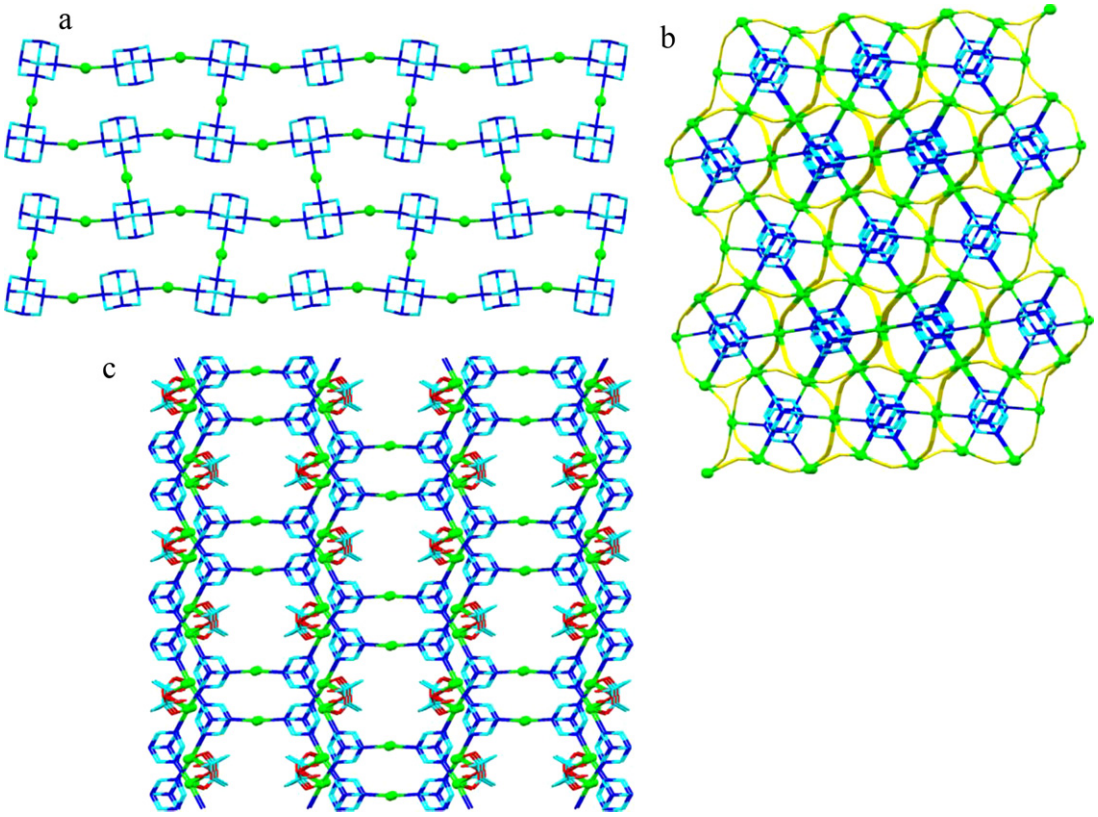

Fig. 6. Simplified structural fragments of **65** [65] (a, b) and **67** (c) [30]: (a) a "brick wall" 2D skeleton from Cd-hmt interactions (view along the *a* axis); (b) an array of the $[Cd_6(\mu\text{-}CN)_6]_n$ "nanotubes" filled with μ_3-hmt moieties (arbitrary view, CN groups are colored in yellow); (c) a 3D network formed via junction of the 2D honeycomb-like $[Cd_6(\mu_3\text{-hmt})_6]_n$ layers (view along the *c* axis). H atoms, H_2O and SO_4^{2-} are omitted for clarity.

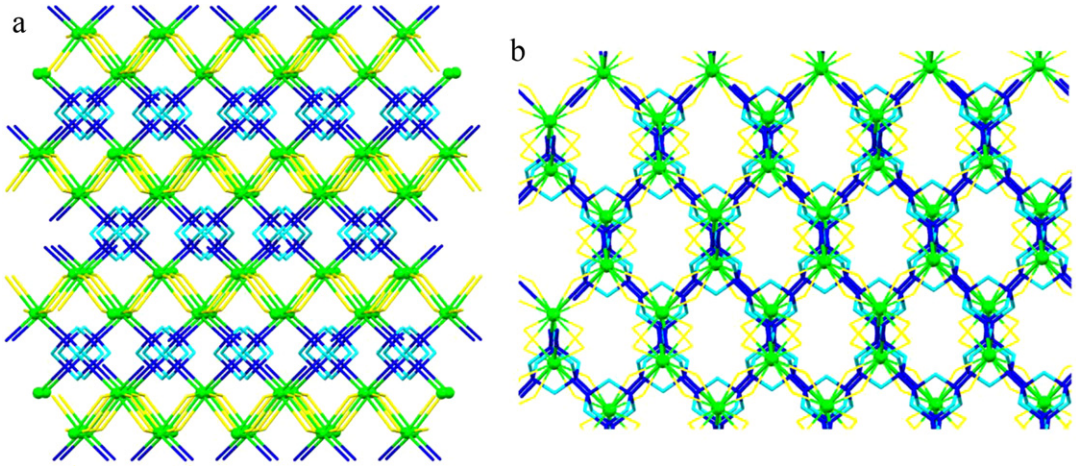

Fig. 7. Structural fragments of **46** [37] showing a quadruple linkage of the 1D ~Hg–$(Cl)_2$–Hg–$(Cl)_2$~ zigzag motifs by μ_4-hmt into a 3D honeycomb-like network ((a) – view along the *a* axis; (b) – arbitrary view). H atoms are omitted for clarity.

(Fig. 4a). Besides, the framework is further reinforced through additional μ-Cl interactions [22]. Another example concerns a compound **66** [63] that adopts "parquet floor" topology [2k] from the tiled rectangular $Hg_6(\mu_3\text{-hmt})_6$ bricks (Fig. 4b). Interestingly, an additional 3D motif can be identified in **66**, which arises from extensive interactions of Hg atoms with μ-Cl and μ-NCS ligands.

In 2005, Zhu and Qiu with co-workers reported [29] the crystal structure of a compound **57**, which is the most complex example within the hmt-driven coordination polymers so far obtained. This compound possesses the unique open framework with the zeolite MTN topology, being defined by the combination of two types of 5^{12} and $6^4.5^{12}$ cages. The small 5^{12} cages are built from twelve $Cd_5(hmt)_5$ pentagons, while big $6^4.5^{12}$ cages also comprise four $Cd_6(hmt)_6$ hexagons [29] (Fig. 5). In addition, **57** is constructed from simple chemicals and represents a rare type of cationic framework.

The sub-group B3 comprises six coordination polymers that are based on hmt-driven 2D layers (**65**, **67**, **69**) or 1D chains (**42**, **44**, **72**) extended to overall 3D networks (except **44**) by means of other bridging ligands. Hence, the structure of $[Cd_3(\mu_2\text{-}CN)_6(\mu_3\text{-hmt})_2]_n$ (**65**) features the formation of 2D undulating layers composed of tiled $Cd_6(\mu_3\text{-hmt})_6$ bricks [65]. Although these

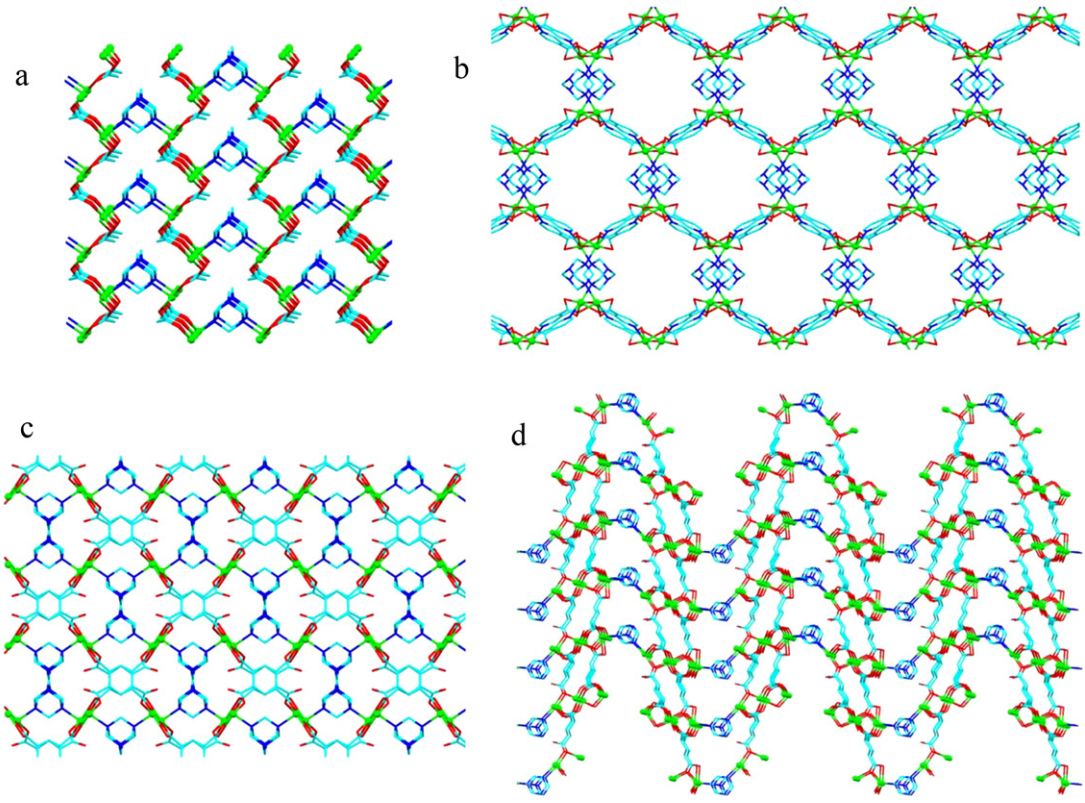

Fig. 8. Selected examples of layer-pillared 3D networks in **49** (a) [33], **43** (b) [17], **54** (c) [39] and **61** (d) [32]. Views are along the *a* (a), *b* (d) and *c* (b and c) axes. H atoms, all coordinated and/or crystallization H_2O, DMF and EtOH molecules are omitted for clarity.

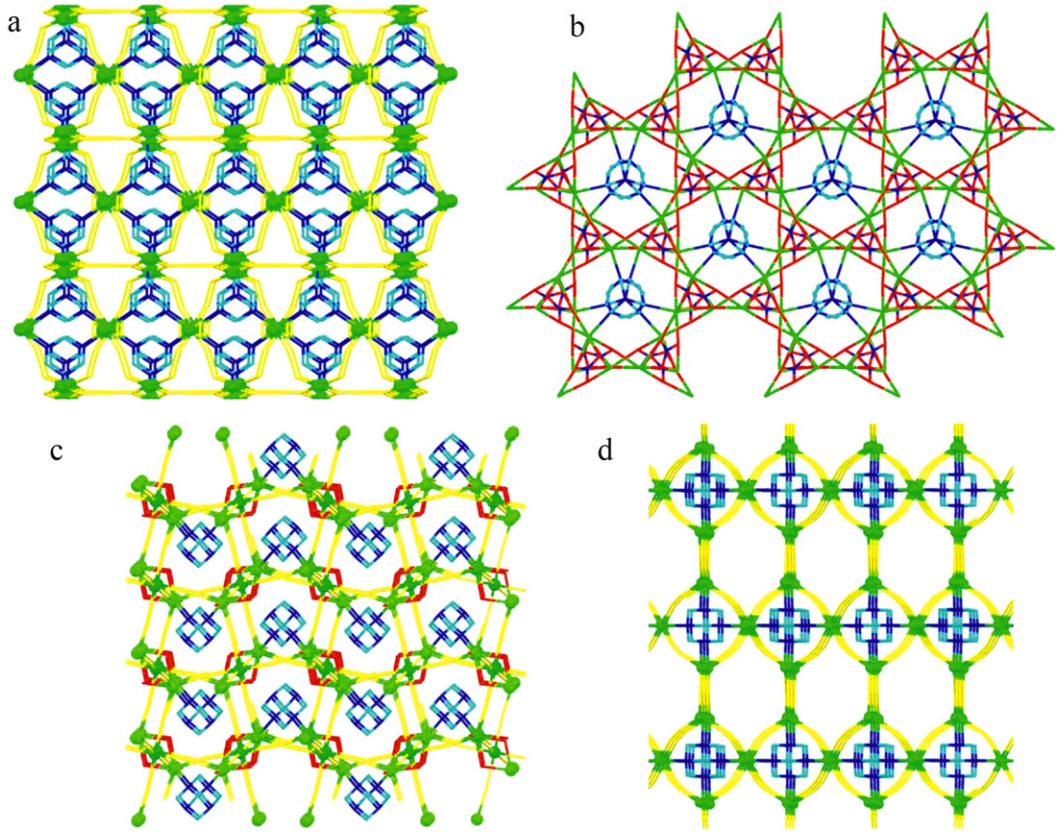

Fig. 9. Examples of 3D metal-organic frameworks reinforced by hmt in **48** (a) [14], **58** (b) [20], **64** (c) [55] and **59** (d) [60]. Views are along the *a* (a and c) and *b* (b and d) axes. H atoms, coordinated (in **48**) and crystallization (in **64**) H_2O molecules are omitted for clarity. For simplicity, Na atoms in **58** are shown as green sticks, while CN groups in **64** and **59** are yellow colored.

bricks resemble those of **66** [63], the topology in **65** is slightly different and can be described [2k] as a "brick wall" (Fig. 6a). These 2D Cd-hmt layers constitute a part of the extended 3D structure formed via multiple cross-linkage of ~Cd–CN–Cd–CN~ motifs [65]. Interestingly, the resulting metal-organic framework can be viewed (Fig. 6b) as an array of the $[Cd_6(\mu\text{-CN})_6]_n$ "nanotubes" filled with μ_3-hmt moieties. A compound $[Cd_3(\mu_2\text{-male})_2(\mu_3\text{-hmt})_2(H_2O)_8]_n(SO_4)_n{\cdot}2nH_2O$ (**67**) [30] comprises flat $[Cd_6(\mu_3\text{-hmt})_6]_n$ layers that adopt honeycomb-like topology, which is similar to that observed e.g. in **40** (Scheme 3, A2). These layers in **67** are interconnected by μ_2-male ligands that act as pillars, furnishing an overall 3D network (Fig. 6c) with the unusual $(6.8^2)(6^4.8.10)$ topology according to Schläfli notation [30]. In $[Cd_4(\mu_2\text{-tar})_4(\mu_4\text{-hmt})(\mu_2\text{-hmt})_2(H_2O)_4]_n{\cdot}8nH_2O$ (**69**) [69], hmt acts as a tetradentate ligand forming the 2D square-grid $[Cd_4(\mu_4\text{-hmt})_4]_n$ layers that are combined into a 3D regular octahedral net by means of μ_2-tar bridging moieties. The topology of the $[Cd_4(\mu_4\text{-hmt})_4]_n$ layers resembles that observed in a compound **47** (see Fig. 4a).

The structure of $[Cd(\mu_3\text{-tcm})(\mu_2\text{-hmt})(H_2O)]_n(tcm)_n$ (**42**) [68] is composed of 1D zigzag Cd-hmt chains (B1 topology, Scheme 2) that are sewed by μ_3-tcm ligands into a 3D octahedral net with rutile-like topology. In $[Cd_2(\mu_2\text{-tpa})_2(\mu_2\text{-hmt})_2(H_2O)_3]_n{\cdot}3nH_2O$ (**44**) [36], μ_2-hmt is bound to Cd atoms forming 1D tooth-shaped zigzag motifs (C1 topology, Scheme 2) that are extended via μ_2-tpa to a second dimension, giving rise to a layered tooth-shaped network. The heterometallic Cd/Na polymer $\{Na[Cd_4(\mu_2\text{-Cl})(\mu_2\text{-dpa})_4(\mu_2\text{-hmt})(hmt)(H_2O)_6]{\cdot}(H_2O)_4\}_n$ (**72**) [25] also possesses 1D tooth-shaped zigzag chains composed of tetracadmium(II) nodes. These chains are extended through μ_2-dpa and μ_4-Na moieties to furnish a 3D network.

The most populated sub-group C3 includes 15 coordination polymers (**43**, **45**, **46**, **49**–**56**, **61**, **62**, **63**, **68**) in which hmt acts as a pillar (or linker) between 0D, 1D or, more typically, 2D metal-organic motifs and extends them to a third dimension. Hence, in an optically active polymer $[Cu_3(\mu_2\text{-pbhd})_3(\mu_3\text{-hmt})]_n$ (**62**) hmt simultaneously connects to three 0D $[Cu_3(\mu_2\text{-pbhd})_3]$ triangular units, giving rise to a highly disordered 10,3-a network arrangement with an anti-clockwise helical twist [26a]. A related highly porous chiral $[Cu_3(\mu_2\text{-bpbpd})_3(\mu_3\text{-hmt})]_n{\cdot}22.5n$THF (**63**) framework was recently reported [26a]. The linkage of 1D mercury(II) halide motifs by either μ_2- or μ_4-hmt was observed in $Hg_2Br_2(\mu_2\text{-Br})_2(\mu_2\text{-hmt})]_n$ (**45**) [42] and $[Hg_2(\mu_2\text{-Cl})_4(\mu_4\text{-hmt})]_n$ (**46**) [37], respectively. The resulting 3D zeolite-like network in **45** possesses similar topology to that of a zeolite Li-A(BW) and can be classified as a $4^2.6^3.8$-a net [42]. In **46**, a rare type of quadruple linkage of the 1D ~Hg–$(Cl)_2$–Hg–$(Cl)_2$~ zigzag chains by μ_4-hmt leads to the generation of a 3D honeycomb-like framework (Fig. 7) that can also be classified as a connected set of puckered 4,4-sheets [37].

Although most of 3D coordination polymers (Table 3) feature rather distinct structures, compounds **49**–**53** are structurally similar, having the general formulae $[M_2(\mu_3\text{-mal})_2(\mu_2\text{-hmt})(H_2O)_2]_n$ {M = Cu (**49**) [33], Co (**50**) [34], Zn (**51**) [33a], Cd (**52**) [40], Mn (**53**) [35]}. This family of compounds is a good example of hmt versatility in the construction of coordination polymers with different metals. All these polymers are composed of the undulating metal-malonate 2D layers that are extended by μ_2-hmt pillars to a 3D framework with $4^4.6^6$ topology (for typical example, see Fig. 8a), which somehow resembles that of 2D layers in **32** and **33** (Scheme 4, E2).

Apart from μ_3-mal moieties, other types of bridging di-, tri- or tetracarboxylate ligands [i.e. 3,4-pyridinedicarboxylate (pdc),

cis,*cis*-1,3,5-cyclohexanetricarboxylate (ctc) or pyromellitate (pma)] were applied for the construction 2D metal-organic layers in $[Cd_2(\mu_3\text{-pdc})_2(\mu_2\text{-hmt})_2(H_2O)_2]_n\cdot 2nDMF\cdot 2nH_2O$ (**43**) [17], $[Cu_2(\mu_4\text{-pma})(\mu_2\text{-hmt})(H_2O)_4]_n\cdot 8nH_2O$ (**54**) [39], $[Mn_2(\mu_4\text{-pdc})_2(\mu_2\text{-hmt})(H_2O)_2]_n$ (**55**) [17], $[Cd_3(\mu_6\text{-ctc})_2(\mu_2\text{-hmt})(DMF)(EtOH)(H_2O)]_n\cdot 3nH_2O$ (**61**) [32] and $[Zn_4(\mu_3\text{-pdc})_4(\mu_2\text{-hmt})(H_2O)_6]_n\cdot 4nDMA\cdot 5nH_2O$ (**68**) [17]. In these compounds, 2D layers are held together by means of μ_2-hmt pillars, resulting in 3D frameworks. In contrast to malonic acid, the use of 3,4-pyridinedicarboxylic acid with different metals led to the generation of distinct coordination polymers **43**, **55** and **68** [17]. Hence, the corrugated 6,3-connected 2D nets in **43** are extended, via μ_2-hmt pillars, to a 3D layer-pillared framework (Fig. 8b) that features hexagonal channels and the overall $(6^3)(6^5.8)$ topology according to Schläfli notation [17]. Other 4,5- and 3,4-connected nets with Schläfli symbols $(4^4.6^2)(4^4.6^6)$ and $(6^3)(6^3.8^3)$ were observed in related Mn(II) and Zn(II) polymers **55** and **68**, respectively [17]. In **54**, the 2D Cu-pma grids are sewed by μ_2-hmt into a 3D network shown in Fig. 8c [39]. An interesting wave-like 3D framework is also formed in **61** (Fig. 8d) from the 6,3-connected Cd-ctc 2D layers that are held together via μ_2-hmt pillars [32].

A compound $[Na_3(\mu_2\text{-}H_2O)_5\{\mu_3\text{-}Fe(CN)_6\}(\mu_2\text{-hmt})(hmt)]_n$ (**56**) [56] represents another example within the sub-group C3, and shows a number of interesting features such as (i) a heterometallic Na/Fe network, (ii) a combination of different coordination modes of hmt, and (iii) unusual $[Na_3(\mu_2\text{-}H_2O)_5]^{3+}$ nodes. Hence, in **56** μ_2-hmt linkers sew adjacent Na/Fe grid-like double layers, resulting in a 3D octahedral network.

The sub-group D3 comprises polymers **48**, **58**–**60**, **64**, **70** and **71** in which hmt only reinforces the already existing 3D metal-organic networks constructed from other ligands. The formation of such compounds is typically observed when using simple inorganic anions (CN^-, N_3^-, NO_3^-) as ligands capable of adopting bridging coordination modes. Hence, the end-to-end and end-on μ_2-bridging azide ligands in $[Co_2(\mu_2\text{-}N_3)_4(\mu_3\text{-hmt})(H_2O)]_n$ (**48**) [14] generate a rare type of complex 3D framework (Fig. 9a) that is further strengthened by μ_3-hmt moieties, resulting in the overall topology resembling that of rutile or pyrite nets [14a]. The Ni(II) compound (**48′**) isostructural to **48** was also reported [14b], although without a single-crystal X-ray analysis. In $[Na_3(\mu_3\text{-}NO_3)_3(\mu_3\text{-hmt})]_n$ (**58**) [20], the sodium and μ_3-nitrate ions form a peculiar 3D framework (Fig. 9b) that possesses nonagonal-like channels filled with the weakly coordinated μ_3-hmt moieties. Although **58** represents the only example of homometallic alkali or alkaline earth metal polymer bearing hmt, the related heterometallic networks were reported in a number of cases, including the Ca/Fe polymer $[Ca_2\{\mu_6\text{-}Fe(CN)_6\}(\mu_2\text{-hmt})(\mu_2\text{-}H_2O)_2]_n\cdot 2nH_2O$ (**64**) [55]. Its structure features an octahedral net skeleton built from the $[Ca_2(\mu_2\text{-}H_2O)_2]^{4+}$ nodes and the μ_6-$Fe(CN)_6$ linkers, which is further stabilized by μ_2-hmt moieties via interactions with the dicalcium nodes forming zigzag hmt-driven 1D motifs (Fig. 9c) [55].

The simple and versatile cyanide ligand is an excellent tool to construct a variety of metal-cyanide clusters and networks [72]. Compounds $[Cd_3(\mu_2\text{-}CN)_6(\mu_4\text{-hmt})]_n$ (**59**) and $[Cd_3(\mu_2\text{-}CN)_5(\mu_3\text{-}OH)(\mu_3\text{-hmt})]_n$ (**60**) [60], $[Cu_5(\mu_3\text{-}CN)_4(\mu_2\text{-}CN)(\mu_4\text{-hmt})]_n$ (**70**) and $[Cu_5(\mu_3\text{-}CN)_4(\mu_2\text{-}CN)(\mu_3\text{-hmt})_2]_n$ (**71**) [18] are quite interesting examples, wherein different Cd(II) or Cu(I) cyanide-driven 3D assemblies are stabilized by μ_3- or μ_4-hmt moieties. Both polymers **59** and **60** show the extended 3D honeycomb-like frameworks that are topologically equivalent but geometrically different [60]. A notable feature of **59** consists in the presence of two types of channels: small tube-like rings filled with μ_4-hmt and larger hexagonal channels that are vacant (Fig. 9d). The very complex topologically distinct 3D networks in **70** and **71** are composed of mono- and dicopper(I) cyanide nodes that connect to additional cyanide groups and bridging hmt moieties [18].

4. Hmt-supported coordination polymers

Although the combination of terminal and bridging hmt ligands has been observed in **27** [21], **56** [56] and **72** [25], the family of polymers wherein hmt acts exclusively as a supporting terminal ligand is limited to four compounds (**73**–**76**) that are summarized in Table 4. Such a small number of examples apparently indicates the preference of hmt for acting as a bridging ligand, thus representing a good building block to design new coordination networks.

The structure of $[Cd(\mu_2\text{-NCS})_2(hmt)(H_2O)]_n\cdot nH_2O$ (**73**) [36,62] reveals the linear NCS-driven 1D chains that are similar to the legs encountered in **25** (Fig. 1b) which, however, are not connected in **73**. Nevertheless, the extension of these chains is achieved via H-bonds between crystallization water and hmt, giving rise to a 2D supramolecular network [36,62]. A compound $\{[hmtH]_2[Pb_3I_2(\mu_3\text{-}I)_2(\mu_2\text{-}I)_4(hmt)_2]\}_n$ (**74**) [57] features the 1D helical chains constructed from repeating Pb_2 and Pb_4 iodide rings that are supported by terminal iodide and hmt ligands. The charge of this anionic network is balanced by protonated hmtH molecules that are intercalated between the adjacent metal-organic chains. The stabilizing role of hmt is also observed in two cobalt(II) coordination polymers $[Co(\mu_3\text{-dtb})(hmt)]_n$ (**75**) [58] and $[CoK_2(\mu_6\text{-nta})(hmt)(\mu_2\text{-}H_2O)_3]_n\cdot nNO_3$ (**76**) [70] that possess 2D and 3D networks, respectively. An interesting feature of the heterometallic cationic network of **76** concerns the unusual $\{[K_2(\mu_2\text{-}H_2O)_3]^{2+}\}_n$ 1D motifs that act as multiple connectors to the $[Co(\mu_6\text{-nta})(hmt)]^-$ units, thus furnishing a honeycomb-like 3D framework.

5. Synthetic methods and ligand types

The remarkable feature of many coordination polymers bearing hmt consists in their rather simple synthetic procedures, which are usually based on the self-assembly reactions of metal salts with hmt in the presence of various types of auxiliary ligands. These self-assembly reactions typically proceed either in sole water (e.g. syntheses of **7**, **8**, **10**, **18**, **26**, **28**, **32**, **42**, **44**, **51**–**53**, **58**, **65**–**67**, **70**, and **71**) or in water–alcohol mixtures (e.g. syntheses of **5**, **6**, **16**, **17**, **24**, **25**, **30**, **38**, **41**, **46**, **49**, **54**, and **72**), at ambient temperature or with a slight heating, for better solubility of reaction components. The resulting products are crystallized upon slow evaporation in air of reaction mixtures, yielding directly X-ray quality single crystals in the majority of cases. The self-assembly syntheses in an organic solvent (typically MeOH or EtOH) or a mixture of organic solvents were also applied for some compounds (e.g. **4**, **9**, **14**, **15**, **27**, **40**, **48**, **61**, **63**, and **73**). Hmt frequently plays a dual role in the self-assembly reactions, in acting as a main ligand and as an organic base to deprotonate auxiliary ligands (e.g. various mono- and polycarboxylates).

As typical examples of self-assembly in water, the syntheses of 1D $[Cu_4(\mu_2\text{-mal})_4(\mu_4\text{-hmt})(H_2O)_4]_n\cdot 3nH_2O$ (**28**) [34], 2D $[Cd_2(\mu_2\text{-NCS})_4(\mu_2\text{-hmt})(H_2O)_2]_n\cdot nH_2O$ (**32**) [16] and 3D $[Hg_3(\mu_2\text{-}Cl)_4(\mu_2\text{-NCS})_2(\mu_3\text{-hmt})_2]_n$ (**66**) [63] coordination polymers can be described in more detail. These are based on the combination, in aqueous medium at r.t., of a simple metal salt ($Cu(ClO_4)_2\cdot 6H_2O$, $CdSO_4\cdot 8/3H_2O$ or $HgCl_2$) with hmt and the corresponding auxiliary ligand (Na_2mal for **28**, or KSCN for **32** and **66**), followed by filtration and crystallization of the obtained filtrate. Interestingly, the modification of a metal source from $Cu(ClO_4)_2\cdot 6H_2O$ (in **28**) to $Cu(mal)\cdot 2H_2O$ (in **49**) led to the generation of a different 3D polymer $[Cu_2(\mu_3\text{-mal})_2(\mu_2\text{-hmt})(H_2O)_2]_n$ (**49**) [33].

The successful self-assembly syntheses and the coordination networks thereof depend on a variety of the following types of reaction parameters [1,2,5]: (i) a metal source, (ii) an auxiliary

ligand, (iii) stoichiometry (metal-to-hmt and metal-to-auxiliary ligand molar ratios), (iv) pH, (v) solvent composition and concentrations, (vi) temperature, and (vii) an order of mixing the reagents. In general, the distinct coordination polymers can be generated through modification of one or several of the above-mentioned reaction parameters. On the other hand, a slight change of the reaction conditions can hamper the formation of a coordination polymer, resulting in the isolation of discrete metal complexes or compounds with uncoordinated hmt [6].

The recent work of Hong et al. [25] demonstrates how a simple modification of the starting cadmium(II) salt during the self-assembly in the $CdX_2/H_2dpa/hmt/NaOH/H_2O/MeOH$ system (X = NO_3, I, Br, Cl, SCN, ac) led to the generation of very different compounds that range from discrete Cd/Na complexes with non-bridging hmt (when using Cd(II) nitrate, iodide, bromide or thiocyanate) to 2D $[Cd_4(\mu_2\text{-dpa})_4(\mu_2\text{-hmt})_3(H_2O)_5]_n\cdot 10nH_2O$ (**41**) and 3D $\{Na[Cd_4(\mu_2\text{-Cl})(\mu_2\text{-dpa})_4(\mu_2\text{-hmt})(hmt)(H_2O)_6]\cdot(H_2O)_4\}_n$ (**72**) coordination polymers with μ_2-hmt (when using Cd(II) acetate and chloride, respectively) [25]. The reaction stoichiometry is an important factor in the synthesis of distinct 3D polymers $[Cu_5(\mu_3\text{-CN})_4(\mu_2\text{-CN})(\mu_4\text{-hmt})]_n$ (**70**) and $[Cu_5(\mu_3\text{-CN})_4(\mu_2\text{-CN})(\mu_3\text{-hmt})_2]_n$ (**71**), which were obtained through refluxing in water at 80 °C the mixtures of CuCN, KCN and hmt in the 4:2:1 (for **70**) or 2:2:1 (for **71**) molar ratios [18]. Compounds $[Cd(fba)_2(\mu_2\text{-hmt})(H_2O)]_n$ (**16**) and $[Cd(fba)_2(\mu_2\text{-hmt})(H_2O)_2]_n\cdot nH_2O$ (**17**) represent an example of pH-dependent self-assembly [13]. Although they possess rather similar formulae, their structures are different and depend on pH of the reaction solution (i.e. pH ≈ 5 and 6 for **16** and **17**, respectively) during the self-assembly synthesis in $H_2O/MeOH$ [13].

Although most of the synthetic procedures are sensitive to the reaction conditions, some coordination polymers can be obtained through different synthetic pathways. A compound $[Ni(NCS)_2(\mu_2\text{-hmt})(H_2O)_2]_n$ (**8**) represents one of such examples, which is prepared by the self-assembly of Ni(II) nitrate with NaSCN and hmt in water at r.t. [43], or by the controlled hydrothermal synthesis from $NiCl_2$, KSCN and hmt in water at 160 °C [27]. Another example, $[Co_2(\mu_2\text{-}N_3)_4(\mu_3\text{-hmt})(H_2O)]_n$ (**48**), is obtained via treatment of $CoCl_2\cdot 6H_2O$ with NaN_3 and hmt, either by self-assembly in MeOH at r.t. [14b] or by heating (70 °C) and slow controlled cooling (during 2 days) in an aqueous solution of hydrazonic acid [14a]. Three different procedures were reported for the synthesis of $[Mn_2(\mu_3\text{-mal})_2(\mu_2\text{-hmt})(H_2O)_2]_n$ (**53**), which can be obtained by self-assembly from manganese(II) chloride in alkaline aqueous [35a] or water/methanol [35b] solutions, or by a stepwise synthesis from Mn(II) sulfate via an intermediate Mn(II) hydroxocarbonate [33b]. Interestingly, the self-assembly methods employing hmt, malonic acid and different salts of Cu, Co, Zn, Cd and Mn resulted in the structurally similar series of 3D polymers **49**–**53**.

Apart from the simple self-assembly methods (see above) for the synthesis of coordination polymers of hmt, other reported routes (some of them can also be considered as self-assembly) include the following types: a controlled hydrothermal synthesis (for **8**, **10**–**12**) or solvothermal reactions (for **43**, **48**, **55**), layering (for **21**, **22**, **35**, **62**) or slow diffusion (for **34**, **45**, **57**), a stepwise synthesis (for **53**, **59**, **60**, **76**), a ligand exchange (for **29**) and even in situ generation of hmt (for **23**, **36**).

For instance, the layer-pillared 3D polymers $[Cd_2(\mu_3\text{-pdc})_2(\mu_2\text{-hmt})_2(H_2O)_2]_n\cdot 2nDMF\cdot 2nH_2O$ (**43**) and $[Mn_2(\mu_4\text{-pdc})_2(\mu_2\text{-hmt})(H_2O)_2]_n$ (**55**) were generated by solvothermal reactions (50–60 °C) of a metal salt ($CdCl_2\cdot 2.5H_2O$ or $MnCl_2\cdot 4H_2O$) with 3,4-pyridinedicarboxylic acid and hmt, in a mixed solvent (DMF/glycol/H_2O for **43**; or DMF/2-methyl-1-butanol/H_2O for **55**) and in the presence of HCl [17]. Examples of the layering synthetic procedure concern 2D $[Cu_3(\mu_2\text{-pbpd})_3(\mu_3\text{-hmt})]_n$ (**35**) [24] and 3D $[Cu_3(\mu_2\text{-pbhd})_3(\mu_3\text{-hmt})]_n$ (**62**) [26a] polymers that were crystallized upon layering the THF solutions of hmt and $[Cu_2(\mu_2\text{-pbpd})_2]$ or $[Cu_3(\mu_2\text{-pbhd})_3]$, respectively. Slow diffusion techniques were applied for the synthesis of the most intricate metal–hmt networks in $[Cu_2(\mu_2\text{-prop})_4(\mu_4\text{-hmt})(\mu_3\text{-hmt})_2]_n$ (**34**) [41] and $[\{Cd_{34}(\mu_4\text{-hmt})_{17}(H_2O)_{102}\}_n(Cl)_{68n}\cdot 46nH_2O\cdot 68n$DMF (**57**) [29]. Hence, slow diffusion of a MeOH solution of hmt into a solution of $[Cu_2(\mu_2\text{-prop})_4(MeOH)_2]$ (prepared in situ) yielded the crystals of **34** within several days [41]. For the synthesis of **57**, a solution of triethylamine in DMF was allowed to diffuse at r.t. into a mixture of $CdCl_2\cdot 2.5H_2O$ and hmt (10:1) in DMF/EtOH/H_2O (5:3:3) containing HCl, resulting in crystals after standing for one month [29].

The syntheses of $[Cd_3(\mu_2\text{-CN})_6(\mu_4\text{-hmt})]_n$ (**59**) and $[Cd_3(\mu_2\text{-CN})_5(\mu_3\text{-OH})(\mu_3\text{-hmt})]_n$ (**60**) require the stepwise reactions of $Cd(NO_3)_2\cdot 4H_2O$ with NaCN and hmt in water, isolation of an intermediate product, followed by its intricate recrystallization procedure to give either **59** or **60** [60]. Although most of the hmt-driven coordination polymers were prepared from simple metal salts, metal complexes possessing some labile ligands can also be used as starting materials in the ligand-exchange reactions. For example, the treatment of $[Cu(MeCN)_4](ClO_4)$ with tricyanomethane and hmt in MeCN medium yielded the 2D polymer $[Cu(\mu_2\text{-tcm})(\mu_2\text{-hmt})]_n$ (**29**) [44].

The most unusual synthetic procedures reported for hmt-driven coordination polymers involve the in situ generation of hmt, which was observed in the course of the syntheses of $[Co_2Cu_2(CO)_8(\mu_2\text{-hmt})_2]_n\cdot n$THF (**23**) [61] and $[Cu_3(\mu_2\text{-CN})_3(\mu_2\text{-hmt})_2]_n$ (**36**) [59]. Hence, the reaction of $[(NH_3)_2CuCo(CO)_4]$ with methylenediamine dihydrochloride in CH_2Cl_2 in the −20–0 °C temperature range furnished the 1D polymer **23** [61]. Another pathway toward in situ generation and complexation of hmt is based on the treatment of a mixture composed of Cu(II) acetate, concentrated aqueous ammonia, formalin (37%) and water, at 85 °C for 30 h on a boiling water bath, to give a compound **36**. Interestingly, both hmt and cyanide moieties in **36** are derived from ammonia and formaldehyde via redox processes, involving a number of mechanistic steps as suggested by Stocker [59].

The use of aqueous medium for the synthesis of coordination polymers is an important feature not only from the viewpoint of green chemistry, but also due to the common involvement of water as a ligand and/or guest molecule in the resulting compound [6]. These aqueous-medium syntheses can also lead to materials with high affinity for water and/or to rare aqua-soluble coordination polymers [73], thus opening up their specific applications in host-guest chemistry and in aqueous medium homogeneous catalysis. Furthermore, water molecules participate in extensive H-bonding interactions and thus act as additional stabilizers of metal-organic frameworks. In fact, the importance of water is reflected by its presence in the structures of 44 and 21 hmt-containing coordination polymers as a ligand and a lattice solvent, respectively.

However, other ligands apart from hmt and water are required for the construction of coordination polymers. In the majority of cases these auxiliary ligands are anionic and possess rather high ability to act in a bridging mode. The most frequently observed ligands in compounds **1**–**76** follow the trend: halide (16) > thiocyanate (11) > cyanide (8) > malonate (6) > nitrate (3), acetate (3), 3,4-pyridinedicarboxylate (3) (figure in brackets is the number of structures). Some ligands such as azide, isocyanate, 4-formylbenzoate, 2,2′-biphenyldicarboxylate and tricyanomethanide occur only in two structures, while 24 different ligands were applied in a single case, in spite of resulting in unusual 2D (e.g. **30**, **33**–**35**) and 3D (e.g. **54**, **61**–**63**, **67**, **69**) network compounds. These facts apparently point out an underdeveloped character of this chemistry of hmt coordination polymers, which thus has a considerable potential for further development.

In general, the analysis of ligands based on the type of functional group led to the conclusion that various aliphatic or aromatic mono- (ac, adca, dpa, fba, ibut, phac, phca, prop), di- (mal, male, pdc, tar, tpa) and polycarboxylates (ctc, pma) are the most common and thus very promising candidates for the design of hmt-driven coordination polymers. Alternative systems can employ simple halide (Cl, Br, I), thiocyanate and cyanide ligands, which can easily originate from a starting metal salt or auxiliary ligand, and already showed the recognized synthetic uses when combined with hmt. Yet another approach consists in using the predefined multimetal building blocks (cluster nodes) in combination with hmt as a linker. For example, such a method was successfully applied to the assembly of 2D (in **35**) and 3D (in **62** and **63**) networks [24,26] via the hmt-linkage of the $[Cu_2(\mu_2\text{-pbpd})_2]$, $[Cu_3(\mu_2\text{-pbhd})_3]$ or $[Cu_3(\mu_2\text{-bpbpd})_3]$ units.

Considering other cagelike aliphatic amino ligands that are closely related to hmt, one should mention a family of coordination polymers derived from triethylenediamine (dabco) (Scheme 5) [6,74]. This simple ligand typically acts as a μ_2-linker in a variety of metal networks in which, and in contrast to hmt, zinc is the most common metal (over 30 structures), followed by Cu, Ag, Co and Cd (over 45 structures in total) [6]. Although the majority of dabco polymers also bear different bridging and terminal carboxylate ligands, these are usually different from those encountered in hmt networks. However, the 3D $\{(H_3O)_2[Cd_3(\mu_5\text{-ctc})_2(\mu_2\text{-dabco})(H_2O)_2]Cl_2\}_n$ [74i] and 1D $[Cu_3(\mu_2\text{-pbpd})_3(\mu_2\text{-dabco})_3]_n{\cdot}3nEt_2O$ [26a] dabco polymers are related to hmt-driven networks of **61** and **35**, respectively. It is thus expected that future syntheses of new hmt polymers can also be based on the modification of synthetic routes known for dabco derivatives.

Another cagelike ligand, 7-nitro-1,3,5-triaza-adamantane (nita), has recently shown [75] an interesting ionic recognition behavior toward Zn, Cd, Hg, Pb and Ag, resulting also in the isolation and structural characterization of 1D $[HgCl_2(\mu_2\text{-nita})]$ and 3D $[Ag(\mu_2\text{-}NO_3)(\mu_2\text{-nita})]$ coordination polymers. Furthermore, the derivatization of hexamethylenetetramine and the use of its cagelike derivatives (Scheme 5) in the design of coordination polymers should allow the formation of new types of metal-organic networks. In fact, two organometallic Cu(I) 2D networks $[Cu_2Cl(\mu_2\text{-}Cl)_2(\mu_3\text{-alhmt})]$ and $[Cu_2(\mu_2\text{-}Cl)_3(\mu_2\text{-alhmt})]$ driven by N-allyl-hexamethylenetetramine(1+) (alhmt) were reported [76]. It is expected that the synthesis and application of other N-functionalized hmt ligands would deserve further exploration. The cagelike aminophosphine 1,3,5-triaza-7-phosphaadamantane (pta) is nowadays one of the most relevant ligands in aqueous organometallic chemistry [77], application of which as a P,N-linker in the construction of coordination polymers has emerged in recent years [78]. In fact, examples of coordination polymers with pta or its derivatives (ptao and ptas) are already known for Ag, Cu, Ru, Hg, Zn and Cd [78], but the controlled multiple coordination of pta cage still continues to be a synthetic challenge.

6. Structural features and properties

Although the coordination polymers of hmt show rich structural diversity and molecular aesthetics, their applications as functional materials still remain little developed. This can be associated with inferior thermal and solvent stability of some hmt polymers (restricted by the strength of the metal–hmt bonds) in comparison with those bearing aromatic N-donor building blocks. Nevertheless, there is a good number of hmt polymers (mainly 3D and 2D networks) that show high thermal stability. The decomposition of metal-organic skeletons, with an eventual loss of hmt moieties, can only begin at temperatures as high as 295 (in **34** [41]), 290 (in **53** [35a], **70** [18]), 245 (in **57** [29]), 240 (in **71** [25]), 235 (in **32** [16]), or 225 °C (in **51** [33a], **63** [26b]). These elevated decomposition limits are well comparable with those of coordination polymers derived from aromatic N- or O-donor ligands. Interestingly, it was observed [18] that increasing the number of metal centers bound to hmt may result in denser, more highly cross-linked networks, which show rising decomposition temperature. Hence, compounds $[Cu_3(\mu_2\text{-CN})_3(\mu_2\text{-hmt})_2]_n$ (**36**), $[Cu_5(\mu_3\text{-CN})_4(\mu_2\text{-CN})(\mu_3\text{-hmt})_2]_n$ (**71**) and $[Cu_5(\mu_3\text{-CN})_4(\mu_2\text{-CN})(\mu_4\text{-hmt})]_n$ (**70**), comprising μ_2-, μ_3- and μ_4-hmt ligands, begin to lose hmt at 215, 240, and 290 °C, respectively [18]. It should also be noted that as solid hexamethylenetetramine is stable at atmospheric pressure and sublimes at 263 °C [20].

In spite of limited applications of hmt polymers as functional materials, a number of selected compounds show rather interesting properties such as host-guest interactions involving water molecules, high porosity, selective sorption of gases and solvents, ion exchange, molecular magnetism and photoluminescence. More detailed description of these features is given below.

6.1. Water clusters within host matrices of coordination polymers

In recent years, the identification, description and classification of various water clusters and polymeric water assemblies within the structures of diverse crystalline materials have become a blooming research area as attested by the number of publications covering this topic, including the state-of-the-art reviews of Infantes et al. [79], Nangia [80], Supriya and Das [81] and Ludwig [82]. The importance of this research consists in providing a contribution toward understanding the properties of bulk water in its liquid and solid states, and interpretation of water–water interactions and hydration phenomena in physical and materials chemistry, biochemistry, catalysis and supramolecular chemistry, drug design and pharmacology [79–83].

Bearing these features in mind and considering that many coordination polymers are known to act as host matrices for the storage of diverse water assemblies, the H-bonding patterns have been analyzed in the crystal structures of hmt-driven and hmt-supported coordination polymers that comprise at least one crystallization water molecule. This analysis allowed to identify 10 different types

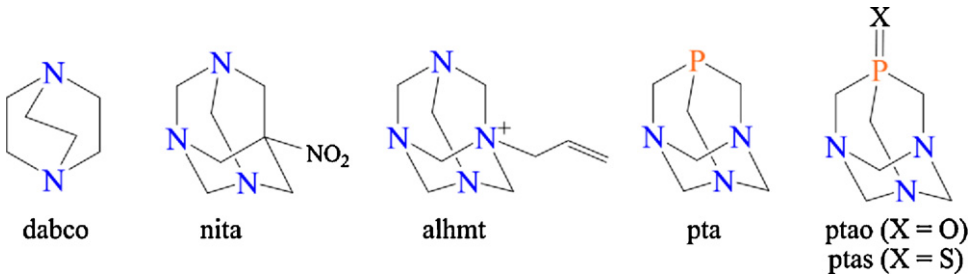

Scheme 5. Cagelike aliphatic amino ligands related to hexamethylenetetramine.

Table 5
Types of water clusters and networks identified in the crystal structures of coordination polymers bearing hmt.

Water cluster/network	Involved $H_2O_{cryst.}/H_2O_{coord.}$	Classification[a]	Compound	Ref.
$(H_2O)_2$	1/1	D2	$[Cd(fba)_2(\mu_2\text{-hmt})(H_2O)_2]_n \cdot nH_2O$ (**17**)	[13]
$(H_2O)_2$	1/1	D2	$[Cd_3I_4(\mu_2\text{-I})_2(\mu_2\text{-hmt})_2(H_2O)_2]_n \cdot 2nH_2O$ (**39**)	[49]
acyclic $(H_2O)_3$	1/2	D3	$[Cd_2(\mu_2\text{-NCS})_4(\mu_2\text{-hmt})(H_2O)_2]_n \cdot nH_2O$ (**32**)	[16]
acyclic $(H_2O)_3$	1/2	D3	$[Cd_3Br_2(\mu_2\text{-Br})_4(\mu_2\text{-hmt})_2(H_2O)_4]_n \cdot 2nH_2O$ (**37**)	[45]
acyclic $(H_2O)_3$	1/2	D3	$[Ca_2\{\mu_6\text{-Fe(CN)}_6\}(\mu_2\text{-hmt})(\mu_2\text{-H}_2O)_2]_n \cdot 2nH_2O$ (**64**)	[55]
acyclic $(H_2O)_4$	3/1	D4	$[Cd_3(\mu_6\text{-ctc})_2(\mu_2\text{-hmt})(DMF)(EtOH)(H_2O)]_n \cdot 3nH_2O$ (**61**)	[32]
cyclic $(H_2O)_4$	2/2	R4	$[Cd(\mu_2\text{-NCS})_2(hmt)(H_2O)]_n \cdot nH_2O$ (**73**)	[36,62]
acyclic polyline-like $(H_2O)_5$	2/3	D5	$[Cd_4Cl_4(\mu_2\text{-Cl})_4(\mu_3\text{-hmt})_2(H_2O)_6]_n \cdot 4nH_2O$ (**31**)	[51]
V-shaped $(H_2O)_5$	3/2	D5	$[Cd_4(\mu_2\text{-tar})_4(\mu_4\text{-hmt})(\mu_2\text{-hmt})_2(H_2O)_4]_n \cdot 8nH_2O$ (**69**)	[69]
cross-like $(H_2O)_5$	3/2	D3A1(2)	$[Cu_4(\mu_2\text{-mal})_4(\mu_4\text{-hmt})(H_2O)_4]_n \cdot 3nH_2O$ (**28**)	[34]
U-shaped $(H_2O)_6$	4/2	D6	$\{Na[Cd_4(\mu_2\text{-Cl})(\mu_2\text{-dpa})_4(\mu_2\text{-hmt})(hmt)(H_2O)_6]\cdot(H_2O)_4\}_n$ (**72**)	[25]
acyclic polyline-like $(H_2O)_9$	6/3	D9	$[Cd_3(ac)_6(\mu_3\text{-hmt})_2(H_2O)_3]_n \cdot 6nH_2O$ (**40**)	[10]
complex $(H_2O)_{16}$[b]	12/4	R4(0)A5(2)A1(2)	$[Cd_4(\mu_2\text{-dpa})_4(\mu_2\text{-hmt})_3(H_2O)_5]_n \cdot 10nH_2O$ (**41**)	[25]
1D $[(H_2O)_6]_n$ branched chain	3/3	C5A1	$[Cd_2(\mu_2\text{-tpa})_2(\mu_2\text{-hmt})_2(H_2O)_3]_n \cdot 3nH_2O$ (**44**)	[36]
1D $[(H_2O)_8]_n$ zigzag chain	6/2	C8	$[Cu_2(\mu_4\text{-pma})(\mu_2\text{-hmt})(H_2O)_4]_n \cdot 8nH_2O$ (**54**)	[39]
1D $[(H_2O)_{11}]_n$ spiral-like branched chain	6/5	T3(0)A4A5	$[Cd_3Br_6(\mu_3\text{-hmt})_2(H_2O)_5]_n \cdot n(hmt) \cdot 6nH_2O$ (**38**)	[12]
Hybrid water contaning clusters				
acyclic $(H_2O)_2(MeOH)$	0/2	–	$[CdBr(NCS)(\mu_2\text{-hmt})(H_2O)_2]_n \cdot n$MeOH (**5**)	[12]
acyclic $(H_2O)_2(MeOH)$	0/2	–	$[CdI(NCS)(\mu_2\text{-hmt})(H_2O)_2]_n \cdot 0.5n$MeOH (**6**)	[12]
acyclic $(H_2O)_5(DMA)$	2/3	–	$[Zn_4(\mu_3\text{-pdc})_4(\mu_2\text{-hmt})(H_2O)_6]_n \cdot 4nDMA\cdot 5nH_2O$ (**68**)	[17]
acyclic $[(H_2O)_3(NO_3)]^-$[c]	0/3	–	$[CoK_2(\mu_6\text{-nta})(hmt)(\mu_2\text{-H}_2O)_3]_n \cdot nNO_3$ (**76**)	[70]
acyclic $[(H_2O)_{11}(SO_4)]^{2-}$[c]	4/7	–	$[Cd_3(\mu_2\text{-male})_2(\mu_3\text{-hmt})_2(H_2O)_8]_n(SO_4)_n \cdot 2nH_2O$ (**67**)	[30]

[a] Classification was performed following the systematization introduced by Infantes et al. [79a].
[b] Independent $(H_2O)_2$ and acyclic $(H_2O)_5$ clusters ($H_2O_{cryst.}/H_2O_{coord.}$ is 1/1 and 4/1, respectively) were also identified within the structure of **41**.
[c] Presence of partial disorder.

of discrete water clusters and 3 types of infinite 1D water chains present in the structures of 17 hmt coordination polymers. Their summary and systematization following the method introduced by Infantes et al. [79a] is given in Table 5, whereas the selected examples are depicted in Figs. 10 and 11. Interestingly, in all the compounds water aggregates are formed through the interactions involving both crystallization and coordinated water molecules, thus additionally contributing to a strong cross-linkage of the metal-organic 1D chains (in **17**, **28**) or 2D (in **31**, **32**, **37**–**41**) layers within 3D supramolecular H-bonded frameworks. The reinforcement of already 3D metal-organic networks via hydrogen bonds through water clusters also occurs in compounds **54**, **61**, **64**, **69** and **72**.

Among the discrete clusters (Fig. 10), water dimers (in **17**, **39** and **41**) and acyclic trimers (in **32**, **37** and **64**) are the most common examples (Table 5). The acyclic and cyclic $(H_2O)_4$ clusters have been found in the structures of **61** and **73**, respectively. Three topologically distinct types of acyclic water pentamers have also been identified, namely including polyline-like (in **31** and **41**), V-shaped (in **69**) and cross-like (in **28**) $(H_2O)_5$ aggregates. The U-shaped $(H_2O)_6$ and acyclic polyline-like $(H_2O)_9$ clusters have been detected within the structures of **72** and **40**, respectively. A compound $[Cd_4(\mu_2\text{-dpa})_4(\mu_2\text{-hmt})_3(H_2O)_5]_n \cdot 10nH_2O$ (**41**) [25] bears 10 crystallization and 5 coordinated water molecules per formula unit, which give rise to the formation of three independent water aggregates, namely the small $(H_2O)_2$ and $(H_2O)_5$ clusters, as well as the large $(H_2O)_{16}$ aggregate. The latter is composed of a "central" cyclic $(H_2O)_4$ core with two pendent water pentamers and two dangling water molecules. The three identified types of infinite 1D water tapes include a branched $[(H_2O)_6]_n$ chain in **44**, a zigzag $[(H_2O)_8]_n$ chain in **54**, and an intricate spiral-like branched $[(H_2O)_{11}]_n$ chain in **38** (Fig. 11).

In contrast to the intensive research on water clusters [79–83], much less attention has been focused on the description of hybrid H-bonded water assemblies with different solvents, small molecules or counterions, in spite of their frequent presence in a variety of crystalline materials [84]. Hence, apart from the above-mentioned water clusters and 1D networks, a few hybrid water associates with other solvents or anions have been identified in coordination polymers of hmt (Table 5). These include the acyclic $(H_2O)_2(MeOH)$ cluster in **5** and **6**, and the $(H_2O)_5(DMA)$ aggregate in **64** that is composed of water dimers and trimers interconnected through a molecule of DMA. In spite of possessing some degree of disorder, the anionic acyclic $[(H_2O)_3(NO_3)]^-$ and $[(H_2O)_{11}(SO_4)]^{2-}$ associates can be observed in the structures of **76** and **67**, respectively.

6.2. Porous materials

Although a considerable number of hmt-driven coordination polymers possess different degrees of porosity, the investigation of gas and/or liquid adsorption or anion exchange properties of such materials remained underexplored, except for compounds $[Cd_2(\mu_3\text{-pdc})_2(\mu_2\text{-hmt})_2(H_2O)_2]_n \cdot 2nDMF\cdot 2nH_2O$ (**43**) [17], $[Cd_2(\mu_2\text{-tpa})_2(\mu_2\text{-hmt})_2(H_2O)_3]_n \cdot 3nH_2O$ (**44**) [36], $[\{Cd_{34}(\mu_4\text{-hmt})_{17}(H_2O)_{102}\}_n(Cl)_{68n} \cdot 46nH_2O \cdot 68n$DMF (**57**) [29] and $[Cu_3(\mu_2\text{-bpbpd})_3(\mu_3\text{-hmt})]_n \cdot 22.5n$THF (**63**), for which some related data has been reported.

Hence, upon removal of guest DMF and H_2O molecules, a compound **43** shows the effective free volume of 42% (0.315 $cm^3\ g^{-1}$) as calculated by PLATON analysis [17]. The methanol adsorption isotherm measured on an "activated" sample of **43** at 20 °C revealed the type I behavior, which is typical for microporous solids. The obtained results suggest that incoming MeOH molecules can easily enter the channels and the 3D framework maintains its rigidity and porosity during the adsorption process [17]. The maximum amount adsorbed by **43** is 87.7 mg/g that corresponds to ca. 8 molecules of MeOH. In contrast to **43**, the related Zn(II) polymer **68** does not maintain porosity upon removal of a crystallization solvent.

The chiral framework of **63** [26b] possesses a significant pore volume (56% estimated by PLATON [17]), which consists of large extended pyramidal voids (9.4 Å diameter) linked by a 3D network of narrow pores (3.9 Å diameter). Although the metal-organic framework of **63** is thermally stable until ca. 225 °C, it contracts significantly upon desolvation of THF. The N_2, Ar and H_2 adsorbtion studies undertaken on a desolvated material $[Cu_3(\mu_2\text{-bpbpd})_3(\mu_3\text{-hmt})]_n$ showed different features. The N_2 sorption at 77 K was atypical, with pronounced hysteresis and a significant step at $0.4P/P_0$ due to the activated gas transport through narrow pore

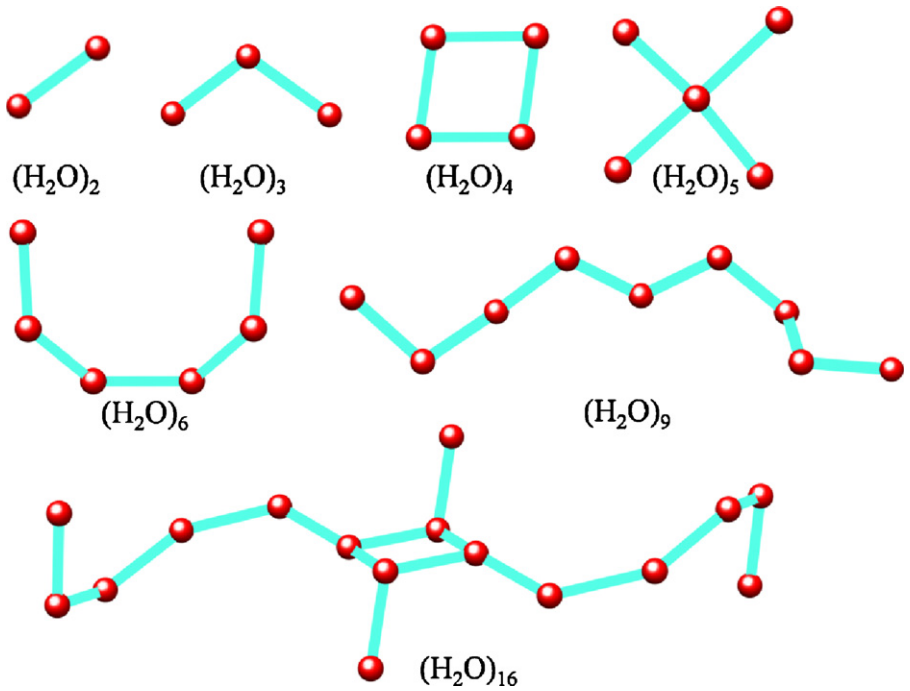

Fig. 10. Selected examples of discrete water clusters [dimer (in **17**, **39**), acyclic trimer (in **32**, **37**, **64**), cyclic tetramer (in **73**), cross-like pentamer (in **28**), U-shaped hexamer (in **72**), acyclic polyline-like nonamer (in **40**) and complex hexadecamer (in **41**)] identified in the crystal structures of hmt coordination polymers (see Table 5 for more details). Water O atoms are shown as red balls, while H-bonds are depicted as solid cyan lines. H atoms are omitted for clarity.

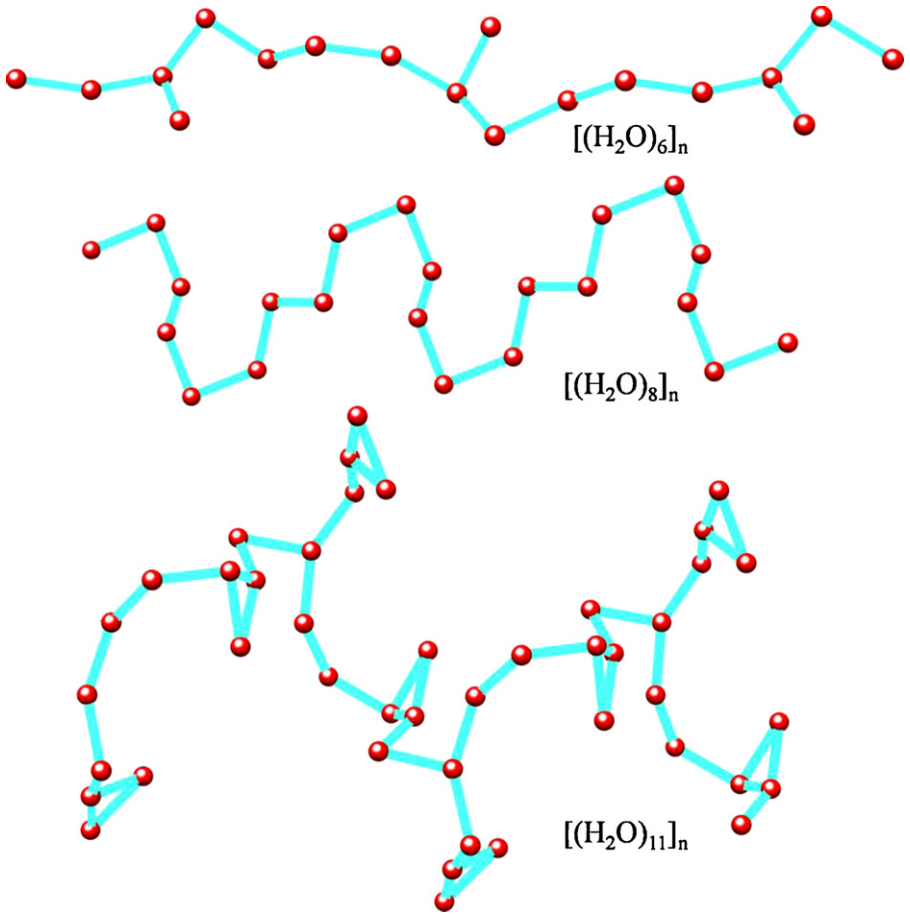

Fig. 11. Examples of infinite 1D water chains [branched $[(H_2O)_6]_n$ (in **44**), zigzag $[(H_2O)_8]_n$ (in **54**) and intricate spiral-like branched $[(H_2O)_{11}]_n$ chain (in **38**)] identified in the crystal structures of coordination polymers (see Table 5 for more details). Water O atoms are shown as red balls, while H-bonds are depicted as solid cyan lines. H atoms are omitted for clarity.

Table 6
Photoluminescent data for selected coordination polymers in the solid state at r.t.

Compound	λ_{em} (nm)	λ_{ex} (nm)	Ref.
$[CdBr(NCS)(\mu_2\text{-hmt})(H_2O)_2]_n \cdot n$MeOH (**5**)	415	330	[12]
$[CdI(NCS)(\mu_2\text{-hmt})(H_2O)_2]_n \cdot 0.5n$MeOH (**6**)	450	330	[12]
$[Cd(fba)_2(\mu_2\text{-hmt})(H_2O)]_n$ (**16**)	480	394	[13]
$[Cd(fba)_2(\mu_2\text{-hmt})(H_2O)_2]_n \cdot nH_2O$ (**17**)	483	394	[13]
$[Cd_2(\mu_2\text{-NCS})_4(\mu_2\text{-hmt})(H_2O)_2]_n \cdot nH_2O$ (**32**)	412, 366 sh.	320	[16]
$[Cd_3Br_6(\mu_3\text{-hmt})_2(H_2O)_5]_n \cdot n(hmt)\cdot 6nH_2O$ (**38**)	450	330	[12]
$[Cd_4(\mu_2\text{-dpa})_4(\mu_2\text{-hmt})_3(H_2O)_5]_n \cdot 10nH_2O$ (**41**)	385	328	[25]
$[Cd_3(\mu_6\text{-ctc})_2(\mu_2\text{-hmt})(DMF)(EtOH)(H_2O)]_n \cdot 3nH_2O$ (**61**)	557	394	[32]
$[Cu_5(\mu_3\text{-CN})_4(\mu_2\text{-CN})(\mu_4\text{-hmt})]_n$ (**70**)	417, 522[a,b]	282, 304	[18]
$[Cu_5(\mu_3\text{-CN})_4(\mu_2\text{-CN})(\mu_3\text{-hmt})_2]_n$ (**71**)	470, 510[a]	285, 302	[18]
$\{Na[Cd_4(\mu_2\text{-Cl})(\mu_2\text{-dpa})_4(\mu_2\text{-hmt})(hmt)(H_2O)_6]\cdot(H_2O)_4\}_n$ (**72**)	418, 496 sh.	340	[25]
$[Cd(\mu_2\text{-NCS})_2(hmt)(H_2O)]_n \cdot nH_2O$ (**73**)	418, 370	338	[62b]

[a] These compounds show a yellow-green (**70**) or yellow (**71**) emission at 298 K, which shifts to blue emission on lowering the temperature to 77 K.
[b] At 4 K, a new shoulder at 451 nm (λ_{ex} = 295 nm) is detected.

windows, whereas the adsorption of Ar at 87 K was about five times greater than that of N_2 [26b]. The adsorption of H_2 at 77 and 87 K was modest. In general, the observed behavior of **63** points out its potential for the use in selective gas separation applications.

The compound **44** was shown to reversibly and selectively readsorb water [36]. It loses all crystallization and coordinated water molecules after heating up to 160 °C. When this dehydrated sample was exposed to air for 2 h, the readsorption of 6 water molecules took place, furnishing the framework material identical to **44** as confirmed by X-ray powder diffraction and thermal analyses. Furthermore, an "activated" sample of **44** is capable of selectively adsorbing water from MeOH or EtOH solutions containing ca. 1% of H_2O, while the adsorption of these alcohols is not possible even when using dry solvents [36]. Such selective adsorption of H_2O can be associated with the dimensions of the channels and the selective H-bonding interactions that lead to the formation of infinite $[(H_2O)_6]_n$ chains (Table 5).

The anion exchange study was undertaken on the cationic zeolite-like polymer **57**, which was subjected to the treatment with KSCN in DMF solution at r.t. The resulting material showed the presence of new SCN moieties and retained the original metal-organic skeleton as confirmed by powder X-ray diffraction [29].

6.3. Molecular magnetism

The variable temperature magnetic susceptibility studies were undertaken for hmt-driven coordination polymers of Cu(II) (**28**, **49**, **54**), Co(II) (**10**, **12**, **48**, **50**), Ni(II) (**8**, **11**), Mn(II) (**53**) and Mn(II)/Mn(III) (**27**). Although bridging hmt moieties are capable of transmitting magnetic interactions, such couplings are typically very weak or even negligible in all the studied examples. However, some other bridging ligands within these compounds (e.g. mal, pma, ibut, azide) can exhibit rather versatile couplings, and thus mediate magnetic interactions.

The very weak antiferromagnetic interactions between metal atoms with the coupling constant (J) ranging from −1.9 to −0.65 cm^{-1} were observed in 1D polymers $[Ni(NCS)_2(\mu_2\text{-hmt})(H_2O)_2]_n$ (**8**) [27], $[Co(NCO)_2(\mu_2\text{-hmt})(H_2O)_2]_n$ (**10**) [19], $[Ni(NCO)_2(\mu_2\text{-hmt})(H_2O)_2]_n$ (**11**) [19a] and $[Co(N_3)_2(\mu_2\text{-hmt})(H_2O)_2]_n$ (**12**) [28], in which monometallic nodes are interlinked via only μ_2-hmt ligands. The global weak antiferromagnetic interactions were also detected in the series of metal-malonate 3D polymers $[M_2(\mu_3\text{-mal})_2(\mu_2\text{-hmt})(H_2O)_2]_n$ {M = Cu (**49**), Co (**50**), Mn (**53**)}, wherein three types of coupling parameters can be taken into consideration [34]: two interactions via carboxylate pathways within 2D M-mal layers (major contribution) and the interlayer interaction through μ_2-hmt pillars (minor contribution). The possible J parameters were assumed to be 0 cm^{-1} (in **50**) [34] or −0.2 cm^{-1} (in **53**) [35b]. Interestingly, the magnetic behavior of the 1D polymer $[Cu_4(\mu_2\text{-mal})_4(\mu_4\text{-hmt})(H_2O)_4]_n \cdot 3nH_2O$ (**28**) composed of tetracopper(II) malonate units and μ_4-hmt linkers reveals the presence of both ferro- and antiferromagnetic interactions, the latter one being dominant [34]. The best fit parameters (J = 13.5 cm^{-1} and J' = −18.1 cm^{-1}) consider only intra-Cu_4 interactions through carboxylate and μ_4-hmt moieties, whereas the coupling constant for intertetramer interactions J'' was close to 0 cm^{-1} [34]. The presence of ferromagnetic interactions between Cu(II) atoms was reported for the 3D polymer $[Cu_2(\mu_4\text{-pma})(\mu_2\text{-hmt})(H_2O)_4]_n \cdot 8nH_2O$ (**54**), in which both μ_4-pyromellitate and μ_2-hmt ligands can transmit magnetic interactions [39].

For a mixed-valent Mn(II)/Mn_2(III) linear-chain polymer $[Mn_3(\mu_3\text{-O})(\mu_2\text{-ibut})_6(\mu_2\text{-hmt})(hmt)]_n \cdot n$EtOH (**27**), the χMT vs. T dependence shows a decreasing feature on cooling from 300 to 1.86 K with the χMT value of 9.25 cm^3 K mol^{-1} at 300 K [21]. The magnetic interactions were modeled using the combination of vector coupling and full-matrix diagonalization methods, resulting in the J values of +11.3, −5.8 and +0.1 cm^{-1}. The latter value reflects the weak coupling between the Mn_3 units through μ_2-hmt which, however, causes the susceptibility below 50 K to differ from that of an isolated manganese trimer [21].

The investigation of magnetic interactions in the 3D polymer $[Co_2(\mu_2\text{-}N_3)_4(\mu_3\text{-hmt})(H_2O)]_n$ (**48**) allowed to identify a new magnetic Co-azide network with unprecedented highly symmetric $(6.8^2)(6^4.10^2)$ topology according to Schläfli notation [14a]. The magnetic features such as a negative Weiss constant, a hysteresis loop at 2K, an abrupt increase in the χMT vs. T dependence below 20 K and the absence of saturation limit [14a], are indicative of spin canted antiferromagnetism, leading to weak ferromagnetism. The magnetic ordering and spontaneous magnetization were observed below Curie temperature of 15.6 K. The isostructural Ni(II) polymer **48′** is a soft ferromagnet below Curie temperature of 10 K [14b].

6.4. Photoluminescence

The photoluminescent properties of a dozen of coordination polymers bearing hmt have been studied in the solid-state (powder samples) at room temperature (ca. 298 K), and the corresponding data is summarized in Table 6. The majority of luminescent polymers are compounds of Cd(II) (i.e. **5**, **6**, **16**, **17**, **32**, **38**, **41**, **61**, **72** and **73**) that apart from hmt typically bear halide and/or thiocyanate or carboxylate ligands. Two luminescent Cu(I) cyanide networks **70** and **71** were also reported.

The solid-state emission spectra of Cd(II) polymers **5**, **6**, **32**, **38** and **73** that bear halide and/or thiocyanate auxiliary ligands show emission bands with maxima in the 415–450 nm range (λ_{ex} = 320–338 nm), which were assigned to the ligand-to-metal

charge transfer (LMCT) [12,16,62b]. The spectra of **32** and **73** also exhibit a sholder or an extra band at λ_{ex} of 366 or 370 nm, respectively. The strong emission bands were also observed in the spectra of Cd(II) polymers **41** (λ_{em} = 385 nm) [25], **61** (λ_{em} = 557 nm) [32] and **72** (λ_{em} = 418 + 496 sh. nm) [25] that comprise bridging di-(dpa) or tricarboxylate (ctc) ligands (Table 6). These LMCT emissions are more intense than those exhibited by uncoordinated 2,2′-biphenyldicarboxylic or *cis,cis*-1,3,5-cyclohexanetricarboxylic acids. Although polymers **41** and **72** consist of similar $\{Cd_4(\mu_2\text{-dpa})_4\}$ cores, they exhibit distinct purple or blue emissions, respectively [25]. Such a difference can be associated with the presence of μ_2-Cl moieties in **72**. In contrast to **41**, **61** and **72**, compounds **16** and **17** show ligand-based emissions (λ_{em} = 480 and 483 nm, respectively) that are less intense and are slighly shifted in comparison with uncoordinated 4-formylbenzoic acid [13].

The 3D copper(I) cyanide coordination polymers **70** and **71** also feature strong luminescence in the solid-state at ambient temperature, showing two emission bands [18]. A high energy (HE) band is observed at λ_{em} of 417 and 470 nm in the spectra of **70** and **71**, respectively, whereas a second low energy (LE) band is detected in the 510–522 mn range (Table 6). Interestingly, both compounds are thermochromic and show either yellow-green (**70**) or yellow (**71**) emissions, which shift to blue emissions on lowering the temperature to 77 K. Such a color change at low temperature is due to a significant increase in intensity of the HE band with concomitant partial dissaperance of the LE band [18]. This behavior can be explained by the energy transfer between the high-energy and low-energy sublatices. In general, the photoluminescence in **70** and **71** is typical for the metal-to-ligand charge transfer behavior based on the large Stokes shift between excitation and emission maxima [18].

7. Conclusions and outlook

The present study has reviewed the main structural and topological types of metal coordination polymers designed using hexamethylenetetramine as a simple, commercially available, water-soluble and highly versatile cagelike building block. In particular, the review has shown that apart from the recognized application of hmt for the engineering of silver-organic networks [5,46], different hmt-driven coordination polymers of other metals (i.e. Cd, Cu, Hg, Co, Zn, Mn, Ni, etc.) can also be easily generated. These coordination polymers feature a high diversity of topologies that include linear, zigzag, double, triple and quadruple 1D chains, rectangular grids, flat and undulating 2D layers, as well as layer-pillared, octahedral, zeolite-like, honeycomb-like and other complex 3D nets, in which hmt acts as a linker or spacer, pillar or connector, stabilizer and/or supporting ligand. Considering the networks driven by dominating metal–hmt interactions, 2D polymers **34** [41], **35** [24], **38** [12] and **40** [10], and 3D polymers **47** [22], **57** [29] and **66** [30] represent the most notable examples.

The work has also overviewed the most common synthetic strategies for the coordination polymers of hmt, which frequently employ facile self-assembly reactions in aqueous medium and use rather simple chemicals. Being dependent on a variety of reaction parameters, the self-assembly methods are often affected by serendipity and difficulties in controlling both the coordination number of hmt and the type of resulting metal-organic frameworks. Other routes such as a controlled hydrothermal synthesis or solvothermal reactions, layering or slow diffusion methods, a stepwise synthesis, ligand exchange and even in situ generation of hmt, have also been reported in a number of cases. In addition, the most common auxiliary ligands (i.e. halide, thiocyanate, cyanide, malonate, nitrate, acetate, 3,4-pyridinedicarboxylate) used for the construction of hmt-driven coordination polymers have been identified which, in the majority of cases, are anionic and tend to adapt a bridging coordination mode. Water is also a very common auxiliary ligand present in many hmt polymers. The solubility of hmt in water and the use of self-assembly syntheses in aqueous medium can lead to materials with high affinity for water, or to rare aqua-soluble coordination polymers, thus opening up their specific applications in e.g. host-guest chemistry, homogeneous catalysis and medicinal chemistry.

The ligand analysis based on the type of functional group allowed the selection of different aliphatic and/or aromatic mono- or polycarboxylates, as well as simple halide, thiocyanate or cyanide ligands as the most promising candidates for future engineering of metal-organic networks with hmt. Given the importance and versatility of different polycarboxylate ligands in the current chemistry of coordination polymers [1,2], it is believed that new functional metal-organic networks composed of hmt and polycarboxylates as building blocks would be designed. In fact, such types of compounds have already shown remarkable porosity (**43**, **44**, **63**), selective sorption of solvents (**43**, **44**) and gases (**63**), and photoluminescent properties (**41**, **61**, **72**). The hmt polymers bearing cyanide or azide moieties also feature notable molecular magnetism (**48**) and photoluminescence (**70**, **71**).

Although the use of hmt as a convenient building block for the design of coordination polymers is still less common than the application of other simple N-donor ligands [3,6], it is expected that this area of research will grow rapidly in the near future. Hence, further developments should focus on (i) the search for new and the modification of currently used auxiliary ligands and/or synthetic procedures for the synthesis of hmt-driven coordination polymers with tunable topologies, (ii) widening the spectrum of metals and extending the still limited family of heterometallic metal-organic networks, and (iii) the application of other cagelike hmt derivatives in the design of coordination polymers. It is believed that future research on hmt-driven polymers will not only concentrate on widening their structural diversity and molecular aesthetics, but also furnish new metal-organic frameworks with functional properties and advanced applications.

Acknowledgement

This work has been supported by the Foundation for Science and Technology (FCT), Portugal, through the “Science 2007” program.

References

[1] (a) S.R. Batten, D.R. Turner, S.M. Neville, Coordination Polymers: Design, Analysis and Application, Royal Society of Chemistry, London, 2009;
(b) A.S. Abd-El-Aziz, C.E. Carraher Jr., C.U. Pittman Jr., M. Zeldin (Eds.), Macromolecules Containing Metal and Metal-Like Elements. Vol. 5 Metal-Coordination Polymers, Willey, 2005;
(c) J.L. Atwood, J.W. Steed (Eds.), Encyclopedia of Supramolecular Chemistry, Taylor & Francis, London, 2004.
[2] For selected reviews on coordination polymers, see:
(a) C.B. Aakeröy, N.R. Champness, C. Janiak, CrystEngComm 12 (2010) 22;
(b) K.M. Fromm, J.L. Sagué, L. Mirolo, Macromol. Symp. 291–292 (2010) 75;
(c) J.J. Perry IV, J.A. Perman, M.J. Zaworotko, Chem. Soc. Rev. 38 (2009) 1400;
(d) S. Qiu, G. Zhu, Coord. Chem. Rev. 253 (2009) 2891;
(e) M.J. Zaworotko, Cryst. Growth Des. 7 (2007) 4;
(f) S. Kitagawa, K. Uemura, Chem. Soc. Rev. 34 (2005) 109;
(g) C.N.R. Rao, S. Natarajan, R. Vaidhyanathan, Angew. Chem. Int. Ed. 43 (2004) 1466;
(h) S. Kitagawa, R. Kitaura, S. Noro, Angew. Chem. Int. Ed. 43 (2004) 2334;
(i) C. Janiak, Dalton Trans. (2003) 2781;
(j) S.L. James, Chem. Soc. Rev. 32 (2003) 276;
(k) B. Moulton, M.J. Zaworotko, Chem. Rev. 101 (2001) 1629.
[3] (a) R.L. LaDuca, Coord. Chem. Rev. 253 (2009) 1759;
(b) S. Noro, S. Kitagawa, T. Akutagawa, T. Nakamura, Progr. Polym. Sci. 34 (2009) 240;
(c) A.Y. Robin, K.M. Fromm, Coord. Chem. Rev. 250 (2006) 2127;
(d) K. Biradha, M. Sarkar, L. Rajput, Chem. Commun. (2006) 4169;
(e) B.-H. Ye, M.-L. Tong, X.-M. Chen, Coord. Chem. Rev. 249 (2005) 545.

[4] (a) M.T. Harvey, Further Studies on Phenolic Hexamethylenetetramine Compounds, BiblioBazaar, LLC, 2009;
(b) E. Lück, M. Jager, S.F. Laichena, Antimicrobial Food Additives: Characteristics, Uses Effects, Vol. 2, Springer, 1997;
(c) A.C. Potter, Reactions of Hexamethylenetetramine with Model Phenols: Model Studies Related to Novolac resins, University of Melbourne, School of Chemistry, 1997;
(d) G.R. Maxwell, Synthetic Nitrogen Products: a Practical Guide to the Products and Processes, Kluwer Academic/Plenum Publishers, 2004;
(e) K. Eller, E. Henkes, R. Rossbacher, H. Höke, Amines, "Aliphatic" in Ullmann's Encyclopedia of Industrial Chemistry, Wiley-VCH Verlag, Weinheim, 2005;
(f) N. Blazevic, D. Kolbah, B. Belin, V. Sunjic, F. Kajfez, Synthesis-Stuttgart 3 (1979) 161;
(g) J.M. Dreyfors, S.B. Jones, Y. Sayed, Am. Ind. Hyg. Assoc. J. 50 (1989) 579.
[5] S.-L. Zheng, M.-L. Tong, X.-M. Chen, Coord. Chem. Rev. 246 (2003) 185.
[6] See the Cambridge Structural Database (CSD, version 5.31, Aug 2010): F.H. Allen, Acta Crystallogr. B58 (2002) 380.
[7] For selected examples of molecular adducts with hmt, see:
(a) Q. Shi, Z.-M. Zhang, Y.-G. Li, Q. Wu, S. Yao, E.-B. Wang, Inorg. Chem. Commun. 12 (2009) 293;
(b) A. Trzesowska, R. Kruszynski, Trans. Met. Chem. 32 (2007) 625;
(c) G. Singh, B.P. Baranwal, I.P.S. Kapoor, D. Kumar, R. Frohlich, J. Phys. Chem. A 111 (2007) 12972;
(d) S.C. Manna, A.K. Ghosh, J. Ribas, M.G.B. Drew, C.-N. Lin, E. Zangrando, N.R. Chaudhuri, Inorg. Chim. Acta 359 (2006) 1395;
(e) D. Chopra, P. Dagur, A.S. Prakash, T.N.G. Row, M.S. Hegde, J. Cryst. Growth 275 (2005) e2049;
(f) D.-L. Long, P. Kogerler, L.J. Farrugia, L. Cronin, Dalton Trans. (2005) 1372;
(g) D.-L. Long, P. Kogerler, L.J. Farrugia, L. Cronin, Angew. Chem. Int. Ed. 42 (2003) 4180;
(h) D. Sun, R. Cao, Y. Sun, X. Li, W. Bi, M. Hong, Y. Zhao, Eur. J. Inorg. Chem. (2003) 94;
(i) J. Jiang, M.J. Sarsfield, J.C. Renshaw, F.R. Livens, D. Collison, J.M. Charnock, M. Helliwell, H. Eccles, Inorg. Chem. 41 (2002) 2799;
(j) W. Yan, J. Yu, R. Xu, G. Zhu, F. Xiao, Y. Han, K. Sugiyama, O. Terasaki, Chem. Mater. 12 (2000) 2517.
[8] P.J. Hagrman, D. Hagrman, J. Zubieta, Angew. Chem. Int. Ed. 38 (1999) 2638.
[9] L. Carlucci, G. Ciani, D.M. Proserpio, S. Rizzato, J. Solid State Chem. 152 (2000) 211.
[10] S. Hazra, B. Sarkar, S. Naiya, M.G.B. Drew, A. Frontera, D. Escudero, A. Ghosh, Cryst. Growth Des. 10 (2010) 1677.
[11] J.-J. Wang, Z. Chang, A.-S. Zhang, T.-L. Hu, X.-H. Bu, Inorg. Chim. Acta 363 (2010) 1377.
[12] A. Banerjee, P. Maiti, T. Chattopadhyay, K.S. Banu, M. Ghosh, E. Suresh, E. Zangrando, D. Das, Polyhedron 29 (2010) 951.
[13] Z.-P. Deng, L.-H. Huo, Y.-M. Xu, S. Gao, H. Zhao, Z. Anorg, Allg. Chem. 636 (2010) 2492.
[14] (a) F.A. Mautner, L. Ohrstrom, B. Sodin, R. Vicente, Inorg. Chem. 48 (2009) 6280;
(b) R.-Y. Li, Z.-M. Wang, S. Gao, CrystEngComm 11 (2009) 2096.
[15] P.T. Ndifon, M.O. Agwara, A.G. Paboudam, D.M. Yufanyi, J. Ngoune, A. Galindo, E. Álvarez, A. Mohamadou, Trans. Met. Chem. 34 (2009) 745.
[16] Y. Bai, W.-L. Shang, D.-B. Dang, J.-D. Sun, H. Gao, Spectrochim. Acta A 72 (2009) 407.
[17] M. Xue, G. Zhu, H. Ding, L. Wu, X. Zhao, Z. Jin, S. Qiu, Cryst. Growth Des. 9 (2009) 1481.
[18] M.J. Lim, C.A. Murray, T.A. Tronic, K.E. de Krafft, A.N. Ley, J.C. de Butts, R.D. Pike, H. Lu, H.H. Patterson, Inorg. Chem. 47 (2008) 6931.
[19] (a) A. Ray, J. Chakraborty, B. Samanta, S. Thakurta, C. Marschner, M.S. El Fallah, S. Mitra, Inorg. Chim. Acta 361 (2008) 1850;
(b) M.A.S. Goher, M.R. Saber, R.G. Mohamed, A.K. Hafez, F.A. Mautner, J. Coord. Chem. 62 (2009) 234.
[20] A. Trzesowska, R. Kruszynski, J. Coord. Chem. 61 (2008) 2167.
[21] S.G. Baca, I.L. Malaestean, T.D. Keene, H. Adams, M.D. Ward, J. Hauser, A. Neels, S. Decurtins, Inorg. Chem. 47 (2008) 11108.
[22] Y. Chen, Y.-L. Wang, S.-M. Ying, S.-L. Cai, Acta Crystallogr. E63 (2007) m2751.
[23] A.K. Ghosh, D. Ghoshal, M.G.B. Drew, G. Mostafa, N.R. Chaudhuri, Struct. Chem. 17 (2006) 85.
[24] J.K. Clegg, K. Gloe, M.J. Hayter, O. Kataeva, L.F. Lindoy, B. Moubaraki, J.C. McMurtrie, K.S. Murray, D. Schilter, Dalton Trans. (2006) 3977.
[25] R. Wang, D. Yuan, F. Jiang, L. Han, Y. Gong, M. Hong, Cryst. Growth Des. 6 (2006) 1351.
[26] (a) J.K. Clegg, L.F. Lindoy, J.C. McMurtrie, D. Schilter, Dalton Trans. (2006) 3114;
(b) J.K. Clegg, S.S. Iremonger, M.J. Hayter, P.D. Southon, R.B. Macquart, M.B. Duriska, P. Jensen, P. Turner, K.A. Jolliffe, C.J. Kepert, G.V. Meehan, L.F. Lindoy, Angew. Chem. Int. Ed. 49 (2010) 1075.
[27] J. Chakraborty, B. Samanta, A.S. Batsanov, J. Ribas, M.S. El Fallah, S. Mitra, Struct. Chem. 17 (2006) 401.
[28] J. Chakraborty, B. Samanta, G. Rosair, V. Gramlich, M.S. El Fallah, J. Ribas, T. Matsushita, S. Mitra, Polyhedron 25 (2006) 3006.
[29] Q. Fang, G. Zhu, M. Xue, J. Sun, Y. Wei, S. Qiu, R. Xu, Angew. Chem. Int. Ed. 44 (2005) 3845.
[30] Q. Liu, Y.-Z. Li, H. Liu, F. Wang, Z. Xu, J. Mol. Struct. 733 (2005) 25.
[31] W.-G. Lu, H.-W. Liu, C.-H. Peng, X.-L. Feng, Chin. J. Inorg. Chem. 21 (2005) 409.
[32] Q. Fang, G. Zhu, M. Xue, J. Sun, G. Tian, G. Wu, S. Qiu, Dalton Trans. (2004) 2202.
[33] (a) Q. Liu, Y.-Z. Li, Y. Song, H. Liu, Z. Xu, J. Solid State Chem. 177 (2004) 4701;
(b) Y.-Q. Zheng, E.-B. Ying, J. Coord. Chem. 58 (2005) 453.
[34] S. Konar, P.S. Mukherjee, M.G.B. Drew, J. Ribas, N.R. Chaudhuri, Inorg. Chem. 42 (2003) 2545.
[35] (a) Q. Liu, B. Li, Z. Xu, X. Sun, K.-B. Yu, Y.-Z. Li, J. Coord. Chem. 56 (2003) 771;
(b) S. Konar, S.C. Manna, E. Zangrando, T. Mallah, J. Ribas, N.R. Chaudhuri, Eur. J. Inorg. Chem. (2004) 4202.
[36] S. Banerjee, M.G.B. Drew, A. Ghosh, Polyhedron 22 (2003) 2933.
[37] S.R. Batten, A.R. Harris, K.S. Murray, J.P. Smith, Cryst. Growth Des. 2 (2002) 87.
[38] S. Wang, M.-L. Hu, S.W. Ng, Acta Crystallogr. E58 (2002) m242.
[39] R. Cao, Q. Shi, D. Sun, M. Hong, W. Bi, Y. Zhao, Inorg. Chem. 41 (2002) 6161.
[40] Q. Liu, B. Li, Z. Xu, X. Sun, K. Yu, Trans. Met. Chem. 27 (2002) 786.
[41] B. Moulton, J. Lu, M.J. Zaworotko, J. Am. Chem. Soc. 123 (2001) 9224.
[42] L. Pan, N. Zheng, Y. Wu, W. Zhang, X. Wu, Inorg. Chim. Acta 303 (2000) 121.
[43] Y. Zhang, J. Li, M. Nishiura, T. Imamoto, J. Mol. Struct. 520 (2000) 259.
[44] S.R. Batten, B.F. Hoskins, R. Robson, Chem. Eur. J. 6 (2000) 156.
[45] M.-L. Tong, S.-L. Zheng, X.-M. Chen, Acta Crystallogr. C56 (2000) 960.
[46] For recent examples of Ag-hmt coordination polymers, see:
(a) S.-M. Fang, S.-T. Ma, L.-Q. Guo, Q. Zhang, M. Hu, L.-M. Zhou, L.-J. Gao, C.-S. Liu, Inorg. Chem. Commun. 13 (2010) 139;
(b) X.-F. Zheng, L.-G. Zhu, CrystEngComm 12 (2010) 2878;
(c) H. Wu, M.-X. Shang, C.-Y. Zhang, X.-M. Huang, Acta Crystallogr. E66 (2010) m1665;
(d) J.-J. Han, T.-Y. Zhang, L. Geng, Acta Crystallogr. E66 (2010) m111;
(e) Wu, X.-W. Dong, J.-F. Ma, H.-Y. Liu, J. Yang, H.-Y. Bai, Dalton Trans. (2009) 3162;
(f) X.-F. Zheng, L.-G. Zhu, Cryst. Growth Des. 9 (2009) 4407;
(g) G.-L. Zheng, H.-J. Zhang, S.-Y. Song, Y.-Y. Li, H.-D. Guo, Eur. J. Inorg. Chem. (2008) 1756;
(h) C.-S. Liu, Z. Chang, J.-J. Wang, L.-F. Yan, X.-H. Bu, S.R. Batten, Inorg. Chem. Commun. 11 (2008) 889;
(i) G.-L. Zheng, Y.-Y. Li, R.-P. Deng, S.-Y. Song, H.-J. Zhang, CrystEngComm 10 (2008) 658;
(j) F.-F. Li, J.-F. Ma, S.-Y. Song, J. Yang, Y.-Y. Liu, Z.-M. Su, Inorg. Chem. 44 (2005) 9374;
(k) L.-Y. Kong, Z.-H. Zhang, W.-Y. Sun, T.-A. Okamura, N. Ueyama, Russ. Crystallogr. Rep. 50 (2005) 648;
(l) S. Lu, S. Qin, Y. Ke, J. Li, H. Pei, S. Zhou, X. Wu, W. Du, Cryst. Res. Technol. 39 (2004) 89;
(m) D. Sun, R. Cao, W. Bi, X. Li, Y. Wang, M. Hong, Eur. J. Inorg. Chem. (2004) 2144;
(n) S. Qin, S. Lu, Y. Ke, J. Li, S. Zhou, X. Wu, W. Du, Russ. J. Struct. Chem. 45 (2004) 566;
(o) B.F. Abrahams, S.R. Batten, B.F. Hoskins, R. Robson, Inorg. Chem. 42 (2003) 2654.
[47] (a) G.R. Dickinson, A.L. Raymond, J. Am. Chem. Soc. 45 (1923) 22;
(b) R.G.W. Wyckoff, R.B. Corey, Z. Kristallogr. 89 (1934) 462.
[48] J. Pickardt, Acta Crystallogr. B37 (1981) 1753.
[49] (a) J. Pickardt, Z. Naturforsch. B 36 (1981) 1225;
(b) T.C.W. Mak, Z. Kristallogr. Kristallgeom. Kristallphys. Kristallchem. 159 (1982) 247.
[50] B. Viossat, P. Khodadad, N. Rodier, Acta Crystallogr. B38 (1982) 3075.
[51] T.-F. Lai, T.C.W. Mak, Z. Kristallogr. 165 (1983) 105.
[52] J. Pickardt, P. Droas, Bull. Latvian Acad. Sci. Phys. Eng. Sci. 40 (1985) 1756.
[53] T.C.W. Mak, Y.-K. Wu, Inorg. Chim. Acta 104 (1985) 149.
[54] T.C.W. Mak, Y.-K. Wu, Inorg. Chim. Acta 121 (1986) L37.
[55] H.-J. Meyer, J. Pickardt, Z. Naturforsch. B 43 (1988) 135.
[56] H.-J. Meyer, J. Pickardt, Z. Naturforsch. B 43 (1988) 1161.
[57] H. Miyamae, H. Nishikawa, K. Hagimoto, G. Hihara, M. Nagata, Chem. Lett. (1988) 1907.
[58] V. Ganesh, A. Radha, M. Seshasayee, T. Subrahmaniyan, G. Aravamudan, Acta Crystallogr. C46 (1990) 2302.
[59] F.B. Stocker, Inorg. Chem. 30 (1991) 1472.
[60] B.F. Abrahams, B.F. Hoskins, J. Liu, R. Robson, J. Am. Chem. Soc. 113 (1991) 3045.
[61] R. Fuchs, P. Klufers, J. Organomet. Chem. 424 (1992) 353.
[62] (a) J. Pickardt, G.-T. Gong, Z. Naturforsch. B 48 (1993) 23;
(b) J. Lu, H.-T. Liu, D.-Q. Wang, X.-X. Zhang, D.-C. Li, J.-M. Dou, J. Mol. Struct. 938 (2009) 299.
[63] J. Pickardt, G.T. Gong, D. Roleke, Z. Naturforsch. B 49 (1994) 321.
[64] J. Pickardt, G.T. Gong, S. Wischnack, C. Steinkopff, Z. Naturforsch B 49 (1994) 325.
[65] J. Pickardt, G.T. Gong, Z. Anorg, Allg. Chem. 620 (1994) 183.
[66] P.H. Svensson, L.A. Bengtsson-Kloo, H. Stegemann, Acta Crystallogr. C51 (1995) 2289.
[67] J. Pickardt, D. Roleke, Z. Kristallogr, New Cryst. Struct. 212 (1997) 154.
[68] S.R. Batten, B.F. Hoskins, R. Robson, Inorg. Chem. 37 (1998) 3432.
[69] S.W. Ng, Private Communication to the CSD (2004) CCDC 174547.
[70] Z. Chen, F. Liang, X. Tang, M. Chen, L. Song, R. Hu, Z. Anorg, Allg. Chem. 631 (2005) 3092.
[71] C.F. Macrae, I.J. Bruno, J.A. Chisholm, P.R. Edgington, P. McCabe, E. Pidcock, L. Rodriguez-Monge, R. Taylor, J. van de Streek, P.A. Wood, J. Appl. Crystallogr. 41 (2008) 466.
[72] For reviews on cyanometallate materials, see:
(a) B. Sieklucka, R. Podgajny, P. Przychodzen, T. Korzeniak, Coord. Chem. Rev. 249 (2005) 2203;
(b) J.-N. Rebilly, T. Mallah, Struct. Bond 122 (2006) 103;
(c) J.S. Miller, J.L. Manson, Acc. Chem. Res. 34 (2001) 563;

(d) L.M.C. Beltran, J.R. Long, Acc. Chem. Res. 38 (2005) 325;
(e) F. Ricci, G. Palleschi, Biosens. Bioelectron. 21 (2005) 389.
[73] (a) A.M. Kirillov, J.A.S. Coelho, M.V. Kirillova, M.F.C. Guedes da Silva, D.S. Nesterov, K.R. Gruenwald, M. Haukka, A.J.L. Pombeiro, Inorg. Chem. 49 (2010) 6390;
(b) M.V. Kirillova, A.M. Kirillov, M.F.C. Guedes da Silva, A.J.L. Pombeiro, Eur. J. Inorg. Chem. (2008) 3423;
(c) Y.Y. Karabach, A.M. Kirillov, M.F.C. Guedes da Silva, M.N. Kopylovich, A.J.L. Pombeiro, Cryst. Growth Des. 6 (2006) 2200.
[74] For selected recent examples of polymers bearing dabco, see:
(a) S. Furukawa, K. Hirai, K. Nakagawa, Y. Takashima, R. Matsuda, T. Tsuruoka, M. Kondo, R. Haruki, D. Tanaka, H. Sakamoto, S. Shimomura, O. Sakata, S. Kitagawa, Angew. Chem. Int. Ed. 48 (2009) 1766;
(b) H. Chun, H. Jung, J. Seo, Inorg. Chem. 48 (2009) 2043;
(c) H. Chun, J. Am. Chem. Soc. 130 (2008) 800;
(d) K. Uemura, Y. Yamasaki, Y. Komagawa, K. Tanaka, H. Kita, Angew. Chem. Int. Ed. 46 (2007) 6662;
(e) M. Bi, G. Li, J. Hua, Y. Liu, X. Liu, Y. Hu, Z. Shi, S. Feng, Cryst. Growth Des. 7 (2007) 2066;
(f) V.I. Ovcharenko, E.V. Gorelik, S.V. Fokin, G.V. Romanenko, V.N. Ikorskii, A.V. Krashilina, V.K. Cherkasov, G.A. Abakumov, J. Am. Chem. Soc. 129 (2007) 10512;
(g) D. Tanaka, S. Horike, S. Kitagawa, M. Ohba, M. Hasegawa, Y. Ozawa, K. Toriumi, Chem. Commun. (2007) 3142;
(h) S. Horike, R. Matsuda, D. Tanaka, M. Mizuno, K. Endo, S. Kitagawa, J. Am. Chem. Soc. 128 (2006) 4222;
(i) M. Xue, G.-S. Zhu, Q.-R. Fang, X.-D. Guo, S.-L. Qiu, Inorg. Chem. Commun. 9 (2006) 603;
(j) H. Chun, D.N. Dybtsev, H. Kim, K. Kim, Chem. Eur. J. 11 (2005) 3521;
(k) D.N. Dybtsev, H. Chun, K. Kim, Angew. Chem. Int. Ed. 43 (2004) 5033.
[75] A.F.D. de Namor, N.A. Nwogu, J.A. Zvietcovich-Guerra, O.E. Piro, E.E. Castellano, J. Phys. Chem. B 113 (2008) 4775.
[76] V.V. Kinzhibalo, M.G. Mys'kiv, V.N. Davydov, Russ. Coord. Chem. 28 (2002) 927.
[77] For comprehensive reviews on PTA chemistry, see:
(a) J. Bravo, S. Bolãno, L. Gonsalvi, M. Peruzzini, Coord. Chem. Rev. 254 (2010) 555;
(b) A.D. Phillips, L. Gonsalvi, A. Romerosa, F. Vizza, M. Peruzzini, Coord. Chem. Rev. 248 (2004) 955.
[78] (a) C. Lidrissi, A. Romerosa, M. Saoud, M. Serrano-Ruiz, L. Gonsalvi, M. Peruzzini, Angew. Chem. Int. Ed. 44 (2005) 2568;
(b) F. Mohr, L.R. Falvello, M. Laguna, Eur. J. Inorg. Chem. (2006) 3152;
(c) M. Serrano-Ruiz, A. Romerosa, B. Sierra-Martin, A. Fernandez-Barbero, Angew. Chem. Int. Ed. 47 (2008) 8665;
(d) A.M. Kirillov, P. Smoleński, M. Haukka, M.F.C. Guedes da Silva, A.J.L. Pombeiro, Organometallics 28 (2009) 1683;
(e) Ł. Jaremko, A.M. Kirillov, P. Smoleński, A.J.L. Pombeiro, Cryst. Growth Des. 9 (2009) 3006;
(f) A. Lis, M.F.C. Guedes da Silva, A.M. Kirillov, P. Smoleński, A.J.L. Pombeiro, Cryst. Growth Des. 10 (2010) 5244;
(g) B.J. Frost, W.-C. Lee, K. Pal, T.H. Kim, D. VanDerveer, D. Rabinovich, Polyhedron 29 (2010) 2373;
(h) X. Tu, H. Truong, G.S. Nichol, Z. Zheng, Inorg. Chim. Acta 363 (2010) 4189.
[79] (a) L. Infantes, S. Motherwell, CrystEngComm 4 (2002) 454;
(b) L. Infantes, J. Chisholm, S. Motherwell, CrystEngComm 5 (2003) 480;
(c) L. Infantes, L. Fábián, W.D.S. Motherwell, CrystEngComm 9 (2007) 65.
[80] A. Nangia, in: J.L. Atwood, J.W. Steed (Eds.), Encyclopedia of Supramolecular Chemistry—Update, Vol. 1.1, Taylor & Francis, London, 2007, pp. 1–9.
[81] S. Supriya, S.K. Das, J. Cluster Sci. 14 (2003) 337.
[82] R. Ludwig, Angew. Chem. Int. Ed. 40 (2001) 1808.
[83] (a) B.C.R. Sansam, K.M. Anderson, J.W. Steed, Cryst. Growth Des. 7 (2007) 2649;
(b) Y. Wang, T.-A. Okamura, W.-Y. Sun, N. Ueyamahttp, Cryst. Growth Des. 8 (2008) 802;
(c) M.N. Kopylovich, E.A. Tronova, M. Haukka, A.M. Kirillov, V.Y. Kukushkin, J.J.R. Fraústo da Silva, A.J.L. Pombeiro, Eur. J. Inorg. Chem. (2007) 4621;
(d) P.S. Lakshminarayanan, E. Suresh, P. Ghosh, J. Am. Chem. Soc. 127 (2005) 13132;
(e) A. Muller, H. Bogge, E. Diemann, Inorg. Chem. Commun. 6 (2003) 52;
(f) M. Henry, J. Clust. Sci. 14 (2003) 267.
[84] (a) D.L. Reger, R.F. Semeniuc, C. Pettinari, F. Luna-Giles, M.D. Smith, Cryst. Growth. Des. 6 (2006) 1068;
(b) P.S. Lakshminarayanan, E. Suresh, P. Ghosh, Angew. Chem. Int. Ed. 45 (2006) 3807;
(c) R.R. Fernandes, A.M. Kirillov, M.F.C. Guedes da Silva, Z. Ma, J.A.L. da Silva, J.J.R. Fraústo da Silva, A.J.L. Pombeiro, Cryst. Growth Des. 8 (2008) 782;
(d) B. Dey, S.R. Choudhury, P. Gamez, A.V. Vargiu, A. Robertazzi, C.-Y. Chen, H.M. Lee, A.D. Jana, S. Mukhopadhyay, J. Phys. Chem. A 113 (2009) 8626.